REPUBLIC OF TÜRKİYE

YILDIZ TECHNICAL UNIVERSITY

GRADUATE SCHOOL OF SCIENCE AND ENGINEERING

ELECTROSPUN ANTIBACTERIAL POLYMER-METAL COMPOSITES

Elif Nur ARSLAN

MASTER OF SCIENCE THESIS

Department of Bioengineering

Bioengineering Program

Supervisor

Assoc. Prof. Dr. Murat TOPUZOĞULLARI

Co-Supervisor

Prof. Dr. Serap ACAR DERMAN

August, 2023

REPUBLIC OF TÜRKİYE

YILDIZ TECHNICAL UNIVERSITY

GRADUATE SCHOOL OF SCIENCE AND ENGINEERING

ELECTROSPUN ANTIBACTERIAL POLYMER-METAL COMPOSITES

A thesis submitted by Elif Nur ARSLAN in partial fulfillment of the requirements for the degree of MASTER OF SCIENCE is approved by the committee on 14.08.2023 in Department of Bioengineering, Bioengineering Program.

Assoc. Prof. Dr. Murat TOPUZOĞULLARI Yıldız Technical University Supervisor	Prof. Dr. Serap ACAR DERMAN Yıldız Technical University Co- supervisor

Approved By the Examining Committee

Assoc. Prof. Dr. Murat TOPUZOĞULLARI, Supervisor
Yildiz Technical University _____

Assoc. Prof. Dr. Emrah Şefik ABAMOR, Member
Yildiz Technical University _____

Assoc. Prof. Dr. Mehmet ÖZBİL, Member
Gebze Technical University _____

I hereby declare that I have obtained the required legal permissions during data collection and exploitation procedures, that I have made the in-text citations and cited the references properly, that I haven't falsified and/or fabricated research data and results of the study and that I have abided by the principles of the scientific research and ethics during my Thesis Study under the title of "Electrospun Antibacterial Polymer-Metal Composites" supervised by my supervisor, Assoc. Prof. Dr. Murat TOPUZOĞULLARI. In the case of a discovery of false statement, I am to acknowledge any legal consequence.

Elif Nur ARSLAN

Signature

This work was supported by the 2210-C M.Sc. scholarship program of The Scientific and Technological Research Council of Turkey (TUBITAK).

Dedicated to my family

and my best friend

ACKNOWLEDGEMENTS

I would like to express my sincere gratitude to my advisor, Assoc. Prof. Dr. Murat TOPUZOĞULLARI, for igniting my passion for skin tissue engineering. Under his guidance, I had the invaluable opportunity to develop functional wound dressings for distinct therapies aimed at addressing chronic wounds. Throughout the process of constructing this thesis, I am deeply indebted to him for his consistent encouragement and patience. His supervision has been like a compass, guiding me toward my dream field. I would also like to extend my heartfelt appreciation to Prof. Dr. Serap ACAR DERMAN for addressing crucial points and providing invaluable advice and patience throughout the entire thesis. Their support played an instrumental role in shaping the outcome of my work.

Additionally, I am grateful to the team at Inovenso Inc., especially Miralay ALTIPARMAK., for their support in conducting SEM analysis of the polymer nanofiber matrices that I produced. Their assistance greatly contributed to the success of this project.

I am deeply grateful to TÜBİTAK for providing me a scholarship opportunity.

Also, I would like to acknowledge my gratitude to Yıldız Technical University, Department of Bioengineering for providing me access to laboratory facilities. I would also like to acknowledge the "306-307 Biopolymers and Vaccines Laboratory" team, especially Shifa ALHAMVİ, for their unwavering support and assistance throughout my time working on this project.

Eventually, I want to express my heartfelt gratitude to my dear family, whose unwavering love and support have been present in every aspect of my life. They have played an integral role in shaping the person I am today, teaching me invaluable life lessons, and standing by my side as I pursued my dreams and aspirations. Their constant presence has been a source of strength and encouragement, and I am truly grateful for their support.

Elif Nur ARSLAN

TABLE OF CONTENTS

LIST OF SYMBOLS

cm	Centimeter
^{o}C	Degree Celsius
GPa	Dynamic Bayesian Networks - Gigapascal
g	Gram
h	Hours
kV	Kilovolt
l	Liter
MPa	Megapascal
µm	Micrometer
ml	Milliliter
mm	Millimeter
mm/min	Millimeter/Minute
mM	Milimolar
nm	Nanometer
Rpm	Revolutions per minute

LIST OF ABBREVIATIONS

AgNPs	Silver nanoparticles
AIBN	Azobisisobutyronitrile
ASTM	American Society for Testing and Materials
CHR	Chrysin
ECM	Extracellular Matrix
ES	Electrospinning
FTIR	Fourier-transform Infrared Spectroscopy
GPC	Gel Permeation Chromatography
HA	Hyaluronic acid
NF	Nanofibers
NMR	Nuclear Magnetic Resonance
PCL	Polycaprolactone
PDI	Polydispersity Index
PEG	Polyethylene glycol
PLGA	Poly(lactic-*co*-glycolic acid)
PMMA	Polymethyl methacrylate
PS	Polystyrene
PVA	Polyvinyl alcohol
PVDF	Polyvinylidene fluoride
P4VP	Poly(4-vinylpyridine)
SEM	Scanning Electron Microscopy
SF	Silk Fibroin
ZNO NPs	Zinc oxide nanoparticles

LIST OF FIGURES

LIST OF TABLES

ABSTRACT

Electrospun Antibacterial Polymer-Metal Composites

Elif Nur ARSLAN

Department of Bioengineering

Bioengineering Program

Master of Science Thesis

Supervisor: Assoc. Prof. Murat TOPUZOĞULLARI

Co- supervisor: Prof. Serap ACAR DERMAN

Many people suffer from open wounds which are based on cuts, burns, surgery or illnesses (e.g., diabetes, bedsores). In some cases, these wounds can easily become contaminated by various pathogens in the environment, endogenous microbes residing on mucous membranes, or microflora on the skin itself. Contemporary wound dressings lack the ability to effectively mitigate wound contamination. Functional wound dressings have been developed to address this health problems.

In this thesis functionalized nanofiber wound dressing material which incorporates poly(4-vinylpyridine) (P4VP), poly(lactic-*co*-glycolic acid) (PLGA), chrysin, and silver nanoparticles (AgNPs) in different combinations were produced by utilizing the electrospinning technique. The produced nanofiber-based materials were characterized Scanning Electron Microscopy (SEM) and Fourier Transform Infrared Spectroscopy (FTIR), and water absorption studies. In addition, the in vitro biological activity of the produced electrospun materials were evaluated against the *E. coli* Gram (-) and *S. aureus* Gram (+) bacteria and on L929 cell line. The SEM images showed that nanofibers ranging between 300-829 nm were produced without beads and junctions.

The water absorption capacity reached up to maximum 375% depending on the composition of the material. The produced nanofibers exhibited antibacterial activity against *E. coli* and *S. aureus* in which the addition of AgNPs into the nanofiber structure considerably increased the antibacterial efficacy of the nanofibers. The results indicated that AgNPs containing nanofibers showed the highest wound healing effect.

The obtained results demonstrate that the functional wound dressing material holds a viable solution for enhancing the efficiency antibacterial wound healing studies. Furthermore, its potential contribution to the scientific literature is noteworthy.

Keywords: Antibacterial, electrospinning, nanofiber, wound dressing.

ÖZET

Elektro-eğrilmiş Antibakteriyel Polimer-Metal Kompozitleri

Elif Nur ARSLAN

Biyomühendis Anabilim Dalı

Yüksek Lisan Tezi

Danışman: Doç. Dr. Murat TOPUZOĞULLARI

Eş-Danışman: Prof. Dr. Serap ACAR DERMAN

Birçok insan kesik, yanık, cerrahi müdahale ya da hastalık (örn. diyabet, yatak yaraları) sebebiyle oluşan açık yaralardan muzdariptir. Bazı durumlarda, bu yaralar, çevrede bulunan farklı patojen tipleri, mukoza zarlarında yaşayan endojen mikroplar veya cildin kendisinde bulunan mikroflora tarafından kolayca kontamine olabilir. Günümüzde kullanılan yara örtüleri, yaraların kontamine olmasını önleyememektedir. Fonksiyonel yara örtüleri, bu sağlık sorunlarına çözüm bulmak amacıyla geliştirilmiştir.

Bu tezde, poli(4-vinilpiridin) (P4VP), poli(laktik-*ko*-glikolik asit) (PLGA), "chrysin" ve gümüş nanopartiküllerini (AgNPs) farklı kombinasyonlarda içeren fonksiyonelleştirilmiş nanolif yara örtüsü malzemesi, elektro-eğirme tekniği kullanılarak üretilmiştir. Üretilen nanolif tabanlı malzemeler Taramalı Elektron Mikroskopu (SEM) ve Fourier Dönüşüm Kızılötesi Spektroskopisi (FTIR) ile karakterize edilmiş ve su emme çalışmalarına tabi tutulmuştur. Ayrıca, üretilen elektro-eğrilmiş malzemelerin in vitro biyolojik aktivitesi *E. coli* Gram (-) ve *S. aureus* Gram (+) bakterilere karşı ve L929 hücre hattı üzerinde değerlendirilmiştir. SEM görüntüleri, boncuk ve bağlantı noktaları olmadan 300-829 nm arasında değişen nanoliflerin üretildiğini göstermiştir. Su emme kapasitesi malzemenin bileşimine bağlı olarak maksimum %375'e kadar ulaşmıştır.

Üretilen nanolifler, *E. coli* ve *S. aureus*'a karşı antibakteriyel aktivite ve nanolif yapısına AgNP'lerin eklenmesi, nanoliflerin antibakteriyel etkinliğini önemli ölçüde artırmıştır. Sonuçlar, AgNPs içeren nanoliflerin en yüksek yara iyileştirme etkisini gösterdiğini belirtmiştir.

Elde edilen sonuçlar, fonksiyonel yara örtüsü malzemesinin antibakteriyel yara iyileştirme çalışmalarının etkinliğini artırmak için uygun bir çözüm sunduğunu göstermektedir. Ayrıca, potansiyel katkısının bilimsel literatürde dikkate değer olduğu görülmektedir.

Anahtar Kelimeler: Antibakteriyel, elektro-eğirme, nanolif, yara örtüsü.

1
INTRODUCTION

1.1 Literature Review

Injuries occur as a result of any disruption or damage to the normal anatomical structure or function which is caused by a pathological phenomenon, and they are resulted from minor or major complications. After sustaining an injury, the skin needs to undergo repair process for restoring its original functionality. Wound healing is a basic, physiological, and complex process that occurs in all tissues and organs of the body [1], [2]. In addition to the tissue defect, the possibility of an infection is very high due to the susceptibility of the injured area to bacterial attacks which may delay the wound healing process [2].

Because of all these difficulties, there is a considerable amount of study being done on the development and manufacturing of wound dressing materials [3]. Different strategies have been used to create dressing materials with bactericidal activity, including surface functionalization of materials by incorporating different polymers or antibacterial agents (antibiotics, antioxidants, nanoparticles, and natural products) [4]. In this aspect, synthetic or natural polymers have been tried to functionalize such materials [3], [5]. Poly(4-vinylpyridine) (P4VP), polyvinyl alcohol (PVA), PLGA, gelatin, silk fibroin (SF), collagen can be given as examples of polymers that can be used in the production of wound dressing materials [6]–[9]. Liu et al., produced a nanofibrous matrix which is based on combination of PLGA and collagen. They aimed to imitate natural biological structures of the skin and wanted to intend this material for applications in wound dressing and tissue engineering. They reported that the most efficient polymer ratio is 50:50, and the nanofiber diameter is 250 nm. Meanwhile, they suggested the produced matrix acts as an accelerator in early wound healing [10].

Moreover, inherently antibacterial polymers can be used to create materials for wound dressings that have benefits such as antibacterial permanence and cellular compatibility [11]. Alshhab et al. developed new hydrophilic films with controlled physicochemical properties and drug-release behavior that could be used as components in transdermal drug delivery systems. In this manner, they produced polyelectrolyte multilayer (PEC) films consisting of sodium alginate (Na-Alg) and P4VP and loaded with the antibacterial agent ciprofloxacin HCl (CIP.HCl). The researchers discovered that the number of layers and the composition of the outer layer influence the physicochemical properties of the films. The resulting multilayer Na-Alg/P4VP films were thin, transparent, and hydrophilic matrices remained stable in acidic buffer solutions with a pH of up to 4.2. The solubility and swelling characteristics of these films indicated their potential as transdermal drug delivery systems for the healing of skin wounds under acidic conditions. The films demonstrated suitability for loading and controlled release of the antibacterial agent ciprofloxacin HCl. These findings show that Na-Alg/P4VP films can be considered as suitable matrices for transdermal delivery systems and warrant further investigations in this field [6].

In addition to being used directly to create wound dressing materials, antibacterial polymers can be combined with other polymers to form blends or copolymers which improves the biological and physical properties of the material. Several kinds of biodegradable polymers are utilized in this setting. The use of biodegradable polymers has several benefits, including the ability to incorporate pharmaceuticals, the elimination of the need for a subsequent removal procedure, and release of the desired medication over a predetermined period of time [12], [13]. The release of the medicine or nanoparticle combined with the biodegradable polymer will hasten the wound healing process.

The usage of various antioxidants has a good impact on the healing of wounds as well as the medication [14], [15]. Khan et al. created a composite nanofiber (NF) membrane by combining zinc oxide nanoparticles (ZnO NPs) and bioactive PLGA/SF via electrospinning to promote the processing of wound closure, stimulation of angiogenesis, migration of cells, deposition of collagen, and re-epithelialization.

They successfully incorporated ZnO NPs into PLGA/SF-based polymer nanofiber matrix. They found positive morphological characteristics, as well as notable mechanical and thermal stability in the NF membranes [15]. Additionally, they showed that the antibacterial activity of the membranes were improved with the addition of ZnO NPs.

Incorporating silver nanoparticles into the chemical composition is another strategy to provide materials for wound dressings with antibacterial characteristics. Silver nanoparticles (AgNPs) have been identified as antibacterial agents due to their various physical and chemical properties such as environmental friendliness, low volatility, and great thermal stability. These distinctive qualities make silver nanoparticles suitable for use in a variety of industries, particularly in healthcare and pharmaceuticals. AgNPs kill the bacteria by attaching to the bacterial cell wall or membrane. As a result, they successfully lower bacterial infections [16]. In addition, they cause the death of bacterial cells by replacing the hydrogen cation and reducing the membrane permeability [17]. The antibacterial property of AgNPs has been attributed not only to the release of metal ions in solution but also to their low surface-to-volume ratio, which enables them to interact with membranes in nanoscale [18]. Dai et al. produced a highly antibacterial poly(lactic-b-4-vinylpyridine) based copolymer dressing material by adding silver ions. After examining the antibacterial activity of the dressing, they found the antibacterial rate of the material surface as 100% against *E. coli* [19]. It is an important advantage that the dressing material is not only antibacterial but also facilitates an effortless wound healing process. At this point, the incorporation of antioxidants in the composition of the dressing material can allow an effective wound healing process.

Chrysin (5,7-dihydroxyflavone) (CHR) is a natural polyphenol with antioxidant properties found in honey, propolis, various herbs, and fruits such as bitter melon (*Momordica charantia*) or wild Himalayan pear (*Pyrus pashia*). CHR has different properties such as reducing oxidative stress in the organism, antiviral properties against viruses, the ability to alleviate psoriasis-like skin lesions, and anticancer activity, etc. It is thought that inclusion of CHR in the dressing material will be beneficial for the surrounding tissue damage [20].

Deldar et al. fabricated polycaprolactone (PCL)/polyethylene glycol (PEG) and PCL/PEG-Chrysin nanofibers by electrospinning. The diameter distribution of the chrysin-loaded nanofibers was distributed between 250 and 750 nm. The fibers were discovered to be cytocompatible and have cytoprotective properties against human fibroblast cells under oxidative stress. The reduced IL-6, IL-1b, TNF-a, and nitric oxide generation of macrophages seeded on CHR-loaded nanofibers compared to PCL/PEG fibers further evidence to their anti-inflammatory properties. As a result, it has been determined that the suggested natural substance-based nanofibrous mats may be desirable for the development of cutting-edge wound care solutions [21].

Another important factor in the wound healing process is the topography and structure of wound dressing material. The extracellular matrix (ECM) of the human body contains filamentous collagen that makes up the majority of our skin. Hence, it is crucial to develop a wound dressing material that mimics the original skin area. Electrospinning (ES) is a widely used method in the fabrication of nanofiber dressings thanks to its ability to produce micro/nano structure materials that similar to the extracellular matrix [22]. Hyung et al. evaluated the biological performance in vivo of SF based nanofiber membranes. As a result, a higher rate of epithelialization and collagen formation was observed in the produced SF nanomatrices compared to commercially available dressings such as Mediofoam® and medical gauze. Additionally, the generated SF membranes have the ability to modulate the level of inflammatory cytokines (IL-10 and TGF-1) that are important for wound healing [23].

Consequently, although several nanofiber based and antibacterial wound dressings have been studied, antibacterial nanofibrous wound dressings containing both antibacterial agent and natural antioxidants are rare. Therefore, we studied such materials in the context of this thesis.

1.2 Objective of the Thesis

The objective of the thesis is to produce electrospun nanofibers from PLGA and P4VP incorporated with AgNPs and CHR to obtain antibacterial, antioxidant and partially biodegradable wound dressing materials. For this purpose, production, characterization and *in vitro* antibacterial activity, cytocompatibility and wound healing assays were accomplished.

1.3 Hypothesis

In this thesis, inherently antibacterial P4VP and biodegradable PLGA polymers were chosen for the production of functional wound dressing materials to be used in chronic wound treatment. These materials will result in antibacterial, biodegradable and biocompatible wound dressing material. Additionally, the incorporation of CHR and AgNPs helps maintain a balanced oxidative stress level and enhances the antibacterial properties of the dressing material during the wound healing process.

It is expected that the wound dressing material which is produced using the electrospinning method will contribute to the studies of skin tissue engineering applications, thanks to its biocompatibility and antibacterial efficacy.

2
GENERAL INFORMATION

2.1 The Human Skin Anatomy

The typical human skin has a surface area of 1.8 m^2 which accounts for approximately 16% of the body weight. These characteristics make the skin the largest organ in the human body. The skin serves multiple purposes which encompass a range of functions such as a protective shield, exhibiting metabolic activity, safeguarding against water loss, harmful pathogens, and various types of injuries such as those caused by heat, chemicals, and ultraviolet radiation [24]. Moreover, it connects humans to their surroundings by means of numerous nerve endings, facilitating their perception of touch. Also, it plays a vital role in regulating body temperature and supporting metabolic processes, while also aiding in the synthesis of vitamin D [25]. It consists of three parts; dermis, epidermis and hypodermis which are shown in Figure 2.1.

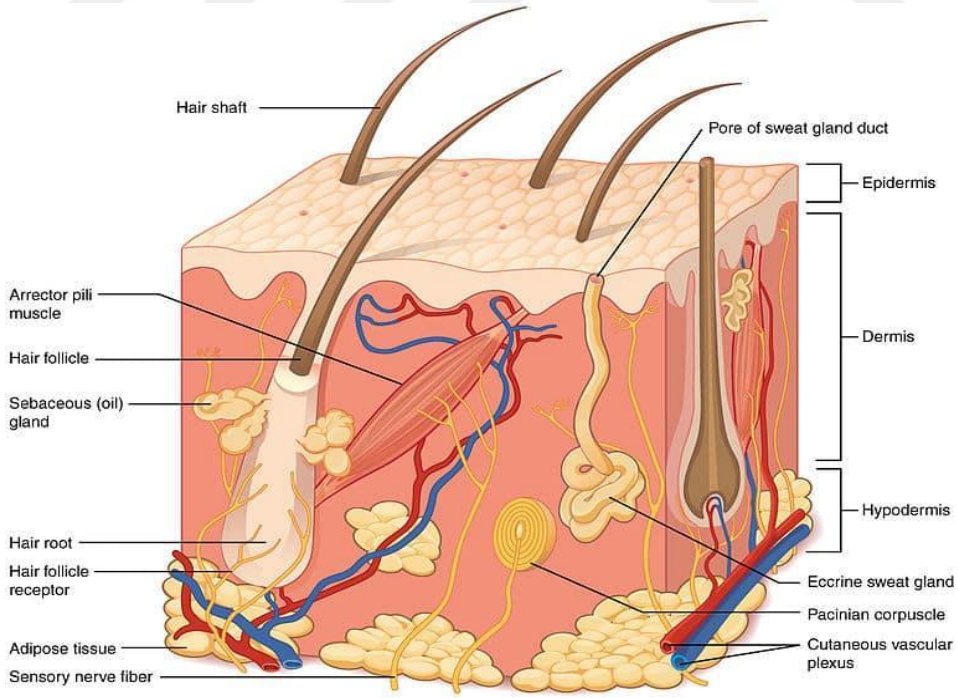

Figure 2.1 The structure of human skin [26]

2.1.1 Epidermis

The epidermis primarily consists of layers of keratinocytes, but it also includes non-epithelial cells such as antigen-presenting dendritic Langerhans cells, melanocytes, and Merkel cells. Nourishment of the epidermis occurs through the diffusion of intercellular fluids originating from the dermal vasculature. This outermost layer of the skin serves as a protective barrier against infections and controls the amount of water released from the body into the atmosphere [27].

2.1.2 Dermis

The dermis, which lies beneath the epidermis, fortifies, and supports the skin by encompassing its vascular, neural, lymphatic, and adnexa components. Serving as a robust foundation, the dermis is capable of absorbing mechanical forces to prevent shearing. It consists of two distinct regions: the superficial papillary zone, composed of relatively thin collagen fibers, and the deeper reticular dermis, characterized by a dense layer of thicker collagen fibers [28].

Within this intricate structure, various sensory cells, sweat glands, nerve endings, capillaries, hair follicles, and touch receptors are located. The dermis assumes vital roles, such as regulating body temperature, maintaining sweat and water balance, shielding against external factors, and detecting sensations of touch, pressure, and pain [29].

2.1.3 Hypodermis

The hypodermis, which is situated between the dermis and the underlying tissues and organs, also known as the subcutaneous layer or superficial fascia. It is composed primarily of adipose tissue, acts as a repository for the body's fat and stores it for future utilization. Moreover, its functions extend beyond fat storage. Since it serves to anchor the skin firmly to the underlying surface, furnishes thermal insulation, absorbs the impact of external shocks upon the skin and shields the body from potential harm [29].

2.2 Human Skin Injuries: Wounds

Any disruption or damage to the typical anatomical structure or function of a human body, which is caused by a pathological event, is referred to as a wound in the dictionary. It is also described as a significant injury to the skin's epidermis in pathology [30]. There are many classifications of wound types in the literature, and their clinical classifications are based on various factors.

Mainly, the number of skin layers and the region of the skin that is affected are examined to classify wounds which are shown in Figure 2.2 [31]. However, they are generally separated into two main groups in the tissue engineering field: acute and chronic etiologies.

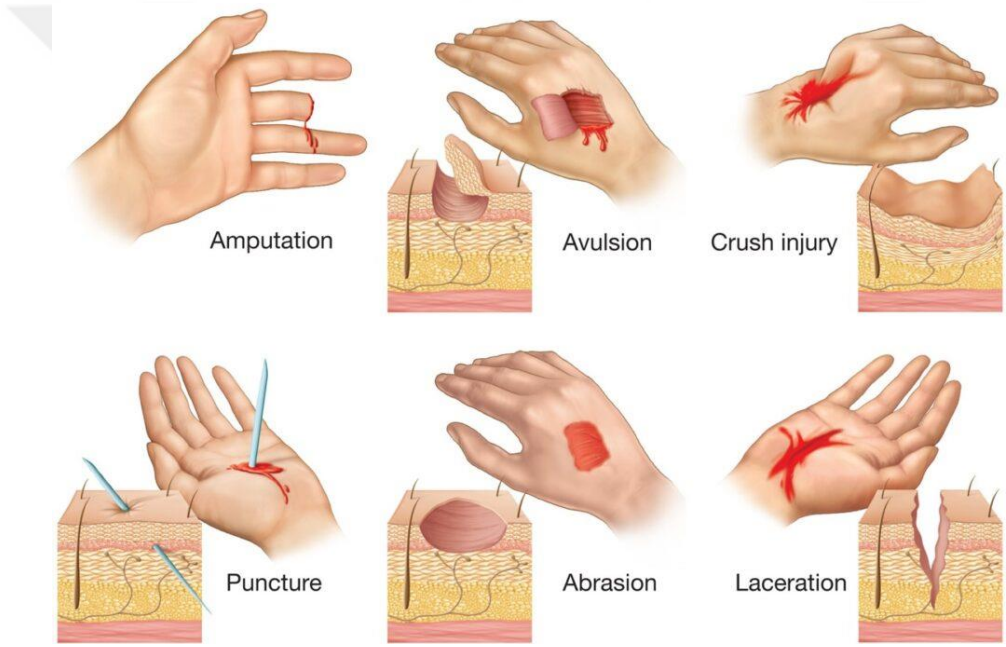

Figure 2.2 Different types of wounds [32]

An acute wound is skin damage that occurs suddenly, rather than gradually. It typically heals the wound at an expected and predictable rate. Acute wounds can happen anywhere on the body and range from minor scrapes to major injuries that harm muscles, blood vessels, and nerves. Examples of acute injuries include abrasions, punctures, crush injuries, heat injuries, gunshots, animal bites, surgeries, and other injuries often caused by trauma. However, the ischemic breakdown can be caused by any process that significantly reduces blood supply to the skin over time [33].

On the other hand, the chronic wound is one that does not heal in the typical orderly stages and within a predicted period of time. These wounds often become trapped in one or more stages of the healing process, like spending too much time in the inflammatory stage. Because of that chronic wounds can take a long time to heal.

There are many kinds of chronic wounds, including venous and arterial ulcers, diabetic ulcers, and pressure ulcers. Some chronic wounds may never fully heal and require years of treatment. Patients who have these wounds often experience excruciating physical and mental suffering. Thus, it is crucial to get the right treatment for them [33]. Except for acute and chronic wounds, there are other types of wound classification which are shown in Table 2.1.

Table 2.1 Classification of wounds [34]

Wound Classification			
The Time of Onset	**The Integrity of Skin**	**The Caused by The Agent**	**The Contamination Status**
Acute Chronic	Open Closed	Chemical Electrical Radiation Thermal Cold	Clean Clean/Contaminated Contaminated Dirty

2.3 Wound Healing Stages

Generally, after the skin is injured, it must be repaired in order to continue its original function. During the repair process, various factors in the body help to drive the complex biological process of wound healing. These factors include cytokines and environmental variables. Cytokines are proteins that allow body cells to communicate with one another. Meanwhile, growth factors, which are subgroups of cytokines, are also involved in the healing process. Through the chemotactic impact of cytokines and growth factors, inflammatory cells and fibroblasts can move to the site of the wound throughout the healing process, stimulating cell proliferation which is represented in Figure 2.3 [35].

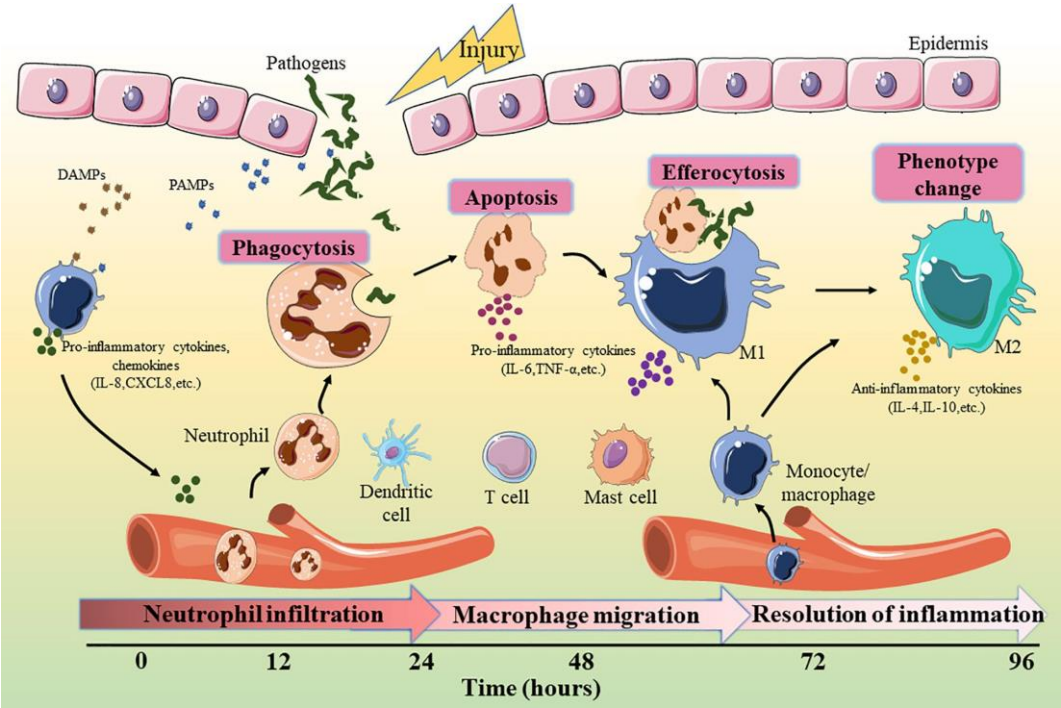

Figure 2.3 Major events that happen during the inflammatory stage of wound healing [35]

Additionally, wound healing is enhanced by promoting angiogenesis and encouraging the development and breakdown of extracellular matrices [36].

Wound healing is a physiological process that is both basic and complex, occurring in all tissues and organs of the body. Biological and immunological systems frequently interact during the healing process. Wound healing is classified into two main groups: acute and chronic. However, chronic wounds continue on for a longer, more complicated period of time without healing, while acute wounds heal within a predicted period of time as mentioned before [37]. Once a wound occurs, the body initiates a complex process of healing that consists of four consecutive and overlapping stages:

- Hemostasis and coagulation starting within the first seconds after skin injury
- Inflammation
- Cell proliferation
- Remodeling in which normal tissue structure is restored

These stages work together to restore the skin's structure and function after injury [37]. In the first phase of wound healing process which is hemostasis and inflammation, cytokines are released to direct the healing process. Hemostasis is achieved when platelets interact with the exposed artery wall of collagen to create a temporary clot. Inflammatory cells then move toward the wound area to remove apoptotic cells and bacteria. This process leads to localized edema, pain, redness, and warmth, which are clinical signs of inflammation observed in the wound area [38].

The wound healing process progresses to the collagen synthesis phase in which a permeable barrier is created, and tissue is strengthened through re-epithelialization and contraction. Fibroblasts synthesize new extracellular matrix and immature Type III collagen, leading to a rapid increase in the wound's resistance to stretching. At the wound edges, epithelial cells from the basal layer form a new surface on the wound [39].

In the last phase of wound healing, which is remodeling, the amount of fibroblasts in the area of the wound is reduced, collagen production reaches equilibrium, and epithelialization is completed. Firmer Type I collagen originates from flexible Type III collagen [39].

The color of the wound area becomes pale, the wound tension resistance increases, and scar tissue is formed. In this manner, the wound healing process is completed. It must be recognized that there are no well-defined orders in wound healing stages; the stages overlap with each other. Additionally, when the quantity of collagen increases, the quantity of fibroblasts decreases [40]. This reverse relationship is depicted in Figure 2.4. It must also be noted that the protection of the wound area from bacteria has the greatest importance in the wound healing process to complete its formal stages [41].

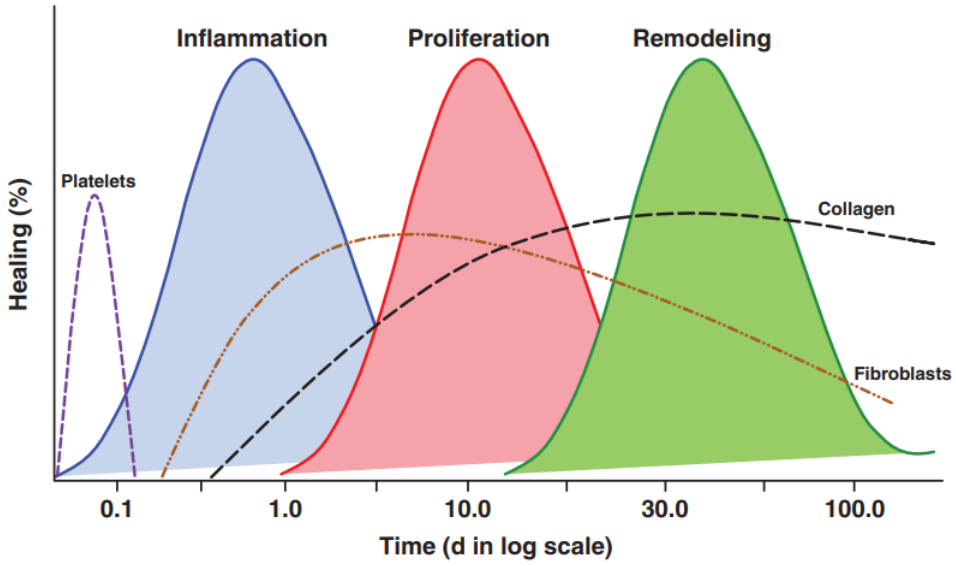

Figure 2.4 Three overlapping steps of the wound-healing process [42]

2.4 Biofilm

Bacterial biofilms are essential for the survival of bacteria and are commonly found throughout nature. In course of time, the significance of biofilms in clinical infections has been widely recognized, and mounting evidence suggests that they play a substantial role in the development and progression of chronic infections. These biofilms consist of clusters of bacteria that attach themselves to surfaces or to each other, forming a structured community embedded in a matrix and produce themselves. The matrix comprises various substances, including proteins like fibrin, polysaccharides like alginate, eDNA and serves as a protective shield [43].

Also, it enables bacteria to employ various survival strategies such as evading the defense mechanisms of their hosts via this layer. Bacteria which form biofilms can inflict local tissue damage, potentially leading to acute infections later by remaining dormant and concealed from the immune system. Within the biofilm structure, bacteria adapt to conditions of low oxygen and limited nutrients by altering their metabolism, gene expression, and protein production. These adaptations result in a decreased metabolic rate and reduced cell division [44].

Moreover, these adjustments render the bacteria highly resistant to antimicrobial therapy. They can inactivate the targets of antimicrobial agents or reduce the dependency on cellular functions that are susceptible to antimicrobials.

In biofilm infections, both the innate and acquired immune responses may be simultaneously activated. However, neither of these immune responses can completely eliminate the biofilm pathogens and, in fact, may accelerate damage to surrounding tissues. As a result, biofilm-related diseases typically manifest as persistent infections that progress slowly, rarely resolve naturally, and exhibit inconsistent responses to antimicrobial treatments and wound healing stages [45].

For this reason, it is crucial to accelerate the wound healing process as the wound is fully exposed to the atmosphere, which harbors numerous microorganisms. Therefore, a new approach has emerged to address this challenge, known as skin tissue engineering. Skin tissue engineering is an engineering field dedicated to reconstructing the structural and functional components of the skin, reducing scar formation, and improving wound healing effectiveness. Taking into consideration the aforementioned concerns, the materials developed in this field, and they are referred to as wound dressing materials [46].

2.5 Wound Dressing Materials

Every year, thousands of people experience various types of skin damage or burns caused by flames, accidents, boiling oil, and water. These injuries can often lead to a disability or even death, and treatment can be costly. Therefore, immediate professional wound care is crucial, regardless of the severity of the wound. There are numerous options for treating the wound in this context, including dressing, bandages, creams, surgery, etc. [47].

In ancient times, healers utilized clay tablets for wound treatment. They would cleanse wounds with milk or water before applying a mixture of resin and honey. Following a period of time, some healers used wine or vinegar to disinfect wounds as an alternative. As the scientific research progresses to the present day, occlusive dressings have been developed to provide a moist environment for wounds, thereby offering protection. These dressings play a crucial role in collagen synthesis, promoting faster re-epithelialization, reducing hypoxia, and maintaining a lower wound bed pH, which in turn reduces the risk of infection [48].

Throughout the years, conventional wound dressings like cotton bandages and gauze tend to absorb a significant amount of moisture from the wound, resulting in excessive drying of the wound surface. Additionally, removing the used dressing material from the injured area can affect the healing rate and make the process more painful. In response to the drawbacks of traditional dressings, a wide variety of polymers have been developed in the form of films, foams, and gels that can provide an optimal condition for the wound healing process which is shown in Figure 2.5. [49]. In the mid-1980s, the concept of modern wound dressing emerged, offering essential features such as maintaining a moist environment and effectively absorbing fluids. In addition, it is also important to choose the type of dressing material according to the type, location, depth, and size of the wound, as well as the level of edema and infection. This breakthrough has greatly improved the treatment of wounds.

Figure 2.5 Types of wound dressings [50]

Apart from the tissue defect, there is a high possibility of infection, which can delay the wound healing process due to the injured area's susceptibility to bacterial attack. To minimize this risk, it is essential to include antibacterial or antioxidant materials in the dressing material to aid the wound healing process [51].

2.5.1 Characteristics of the Wound Dressing Material

There are many parameters that affect the applicability of dressing materials. Determining the appropriate wound dressing selection is crucial for the healthy progress of the wound healing. It is advisable to take into consideration wound-related parameters such as size, color, type, location, and exudate level. An appropriate dressing material should be able to manage moisture around the wound, increase gas exchange, remove excessive exudates, guard against infection and disease-causing organisms, and minimize wound surface necrosis. It is essential to be non-toxic, biocompatible, and biodegradable in functionalized settings like controlled drug release. Additionally, it is recommended to have high mechanical strength and elasticity, be easy to replace, provide pain relief for the wounded area, and have an acceptable cost [48]. The aforementioned details are outlined in Figure 2.6.

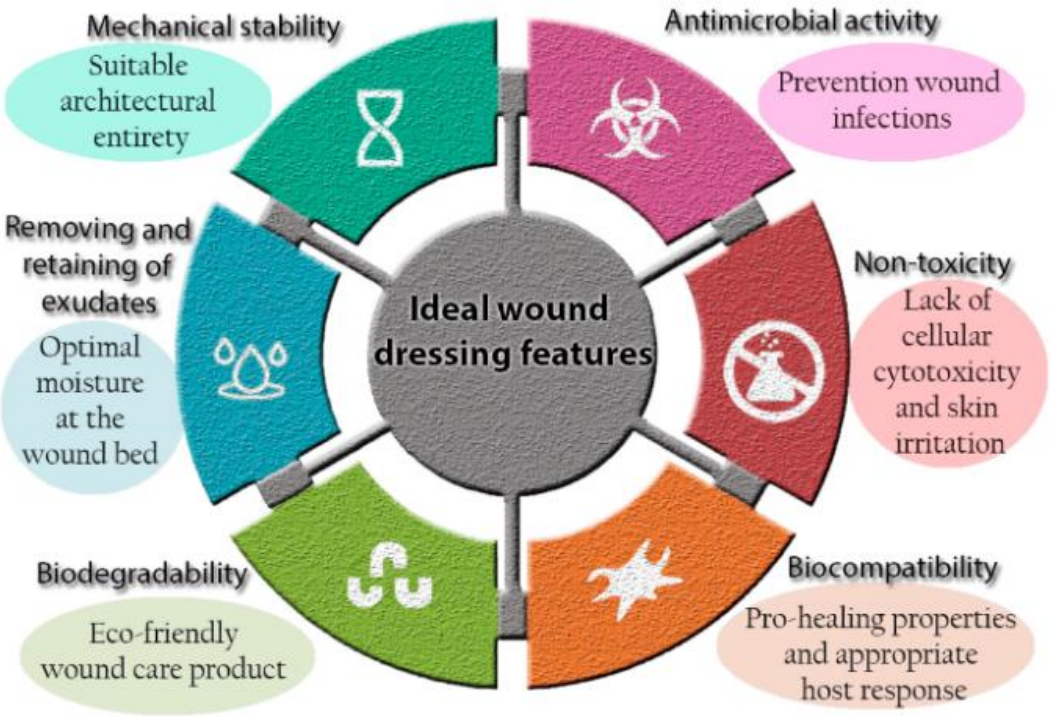

Figure 2.6 Features of ideal dressing material [52]

Among other features, humidity is one of the key factors. Dressing materials with high humidity have greater advantages than materials that lack this feature because the damaged area is susceptible to drying and tension.

The other most influential factor in the characteristic structure of the wound dressings is the material which is used during production. The main materials of wound dressings are polymers. By altering the polymer content or type, it is possible to obtain an ideal wound dressing material with the listed features [53]. In order to ensure the suitability of dressings for soft tissue engineering, their mechanical strength undergoes evaluation through tests such as tensile, compression, and fatigue. Tensile properties are typically evaluated using the standard test procedure outlined in the American Test Standards (ASTM) D882-97 and the optimal elastic modulus value for wound dressings, as specified in the literature, is between 50-120 kPa [54].

Scientists face the formidable task of developing an ideal dressing material that incorporates all of these aforementioned characteristics and try to facilitate an optimal environment for the regenerative process of the wound area. As a consequence, advancements in scientific knowledge have driven the evolution of materials employed in wound dressing production with the aim of creating enhanced conditions for wound healing [55].

2.5.2 Polymer-Based Dressing Materials

Polymer-based wound dressing materials exhibit various fascinating qualities that can be advantageous in the treatment of chronic injuries. Various polymers can be used to create ideal wound dressing materials. They are divided into two types: natural (biopolymers) and synthetic polymers [56].

2.5.2.1 Natural Polymers

Chitin, dextran, alginate, chitosan, hyaluronic acid (HA), cellulose, gelatin, and other natural polymers are examples of biopolymers. These polymers have great biodegradability, good biocompatibility, non-toxicity, hemostatic effects, and wound healing qualities. In addition, some biopolymers exhibit antibacterial efficacy. On the other hand, biopolymers have weak mechanical characteristics [57]. To improve their mechanical performance, natural-based polymeric wound dressing materials are frequently cross-linked or blended with synthetic polymers.

Poly(lactic-co-glycolic acid), poly(ethylene glycol), poly(vinyl alcohol), polyurethanes, polylactide, polyglycolic acid, poly(hydroxyethyl methacrylate), polyvinyl pyrrolidone, and poly(ethylene oxide) are examples of synthetic polymers that are used with natural polymers in wound dressing formulations [58]–[61].

2.5.2.2 Synthetic Polymers

Wound dressing has undergone modernization with time and its main component is synthetic polymers. Dressings which are made from synthetic polymers are separated into two groups: passive and interactive. Passive synthetic polymer dressings are non-occlusive and used to cover wounds and support the recovery of function beneath the polymer coating. Gauze and tulle are examples of such materials. On the other hand, occlusive or semi-occlusive interactive synthetic polymer dressings act as a barrier to prevent bacterial entry into the wound. Examples of this group are hydrogels, foams, and hydrocolloids [62].

In recent years, scientists have concentrated on developing novel polymeric materials that contain antibacterial properties to enhance the wound healing. The antibacterial activity of these polymers mostly depends on electrostatic interaction between positively charged antibacterial polymers and negatively charged bacterial cell walls. Consequently, produced material attaches to the bacteria and minimizes its side-effects [5]. Cationic polymers are inherently antibacterial due their positive charges. P(4-VP), polyhexamethylene biguanide, poly(2-dimethylaminoethyl methacrylate) as cationic polymers are some examples of such polymers [63].

2.5.2.3 Poly(4-vinylpyridine) (P4VP)

P4VP (Figure 2.7) is a polybase with intriguing features derived from the vinyl and aromatic pyridine ring. After the quaternization of nitrogen atoms that are located on the pyridine rings, the polymer becomes positively charged and offer significant benefits for various applications such as the strong affinity of the pyridyl group to metals, hydrogen bonding ability with polar surfaces, and self-antibacterial properties. Therefore, it has the potential to be used in wound dressing materials.

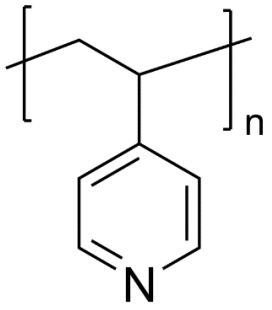

Figure 2.7 Chemical structure of P4VP

The ability of diverse chemistries to modify the nitrogen atoms on repeating units of P4VP-based materials, are critical for advanced materials design [64].

2.5.2.4 Poly(lactic-*co*-glycolic acid) (PLGA)

Polylactide-polyglycolide (PLGA) belongs to a category of synthetic copolymers that are biodegradable and biocompatible. It is commonly used to produce resorbable sutures, surgical clips, and controlled-release implants. These copolymers have been employed in implantable and injectable drug delivery systems with excellent outcomes. It is also FDA-approved and safely used in human populations. Once it is introduced to the human body, PLGA undergoes hydrolysis of its ester linkages via minimal inflammation and lactic-glycolic acids are the side product of it. Furthermore, the biodegradation rate of PLGA is directly proportional to the lactide to glycolide ratio [65]. Electrospinning techniques are often employed to create PLGA nanofiber membranes that possess favorable mechanical properties, controlled degradability, and drug-release capabilities. Despite its numerous advantages, PLGA also exhibits certain limitations in biomedical applications, including inadequate hydrophilicity and cell affinity [10].

2.6 Secondary Active Components Used in Dressing Materials

The copolymerized or cross-linked dressings might have insufficient biological functions and wound-healing abilities, which makes them unsuitable for treating any type of wounds. Therefore, encapsulating secondary active compounds in polymer-based bandages is a potential strategy for treating wounds to promote effective wound healing, especially in chronic wounds [66].

Anti-inflammatory medicines, antibiotics, synthetic nanoparticles, plant extracts, stem cells, growth factors, antioxidants, (such curcumin, etc.), and vitamins are among the bioactive compounds used in wound healing applications. Transdermal patches, foams, hydrogels, films, membranes, nanofibers, and other polymeric wound dressings are examples of those that are loaded with the aforementioned compounds [67].

2.6.1 Synthetic Active Components in Wound Dressing

One of the primary domains of scientific investigation is nanotechnology and its concern the design, production, and manipulation of particles at the nanoscale. The final product of nanotechnology is called nanomaterial and typically possesses at least one exterior dimension or particle size ranging from 1 to 100 nm. Silver, gold, and synthetic polymeric nanoparticles find extensive utilization in wound dressing applications to augment the process of wound healing [68]. Nanoparticles (NPs) exhibit considerable potential in expediting wound healing and contributing to injury treatment. They offer substantial advantages such as antibacterial-microbial activity and minimal side effects. Consequently, they can be utilized to reduce the spread of antibiotic-resistant bacteria. Moreover, NPs have the ability to absorb exudates, function as an antibacterial agent, emulate the ECM structure, and maintain a moist wound environment [69].

2.6.1.1 Silver Nanoparticles

Silver nitrate, known by the chemical formula $AgNO_3$, is a chemical compound utilized extensively in the creation and formulation of various silver compounds such as silver halides and silver oxide. This compound exhibits remarkable reactivity as its nitrate ion which can be substituted by other chemical groups. The reason behind this is that silver is inert in its metallic form, but it is ionized after the reaction. Consequently, it holds significant value as a precursor to numerous silver derivatives, particularly in the fields of nanoscience, medicine and tissue engineering [70].

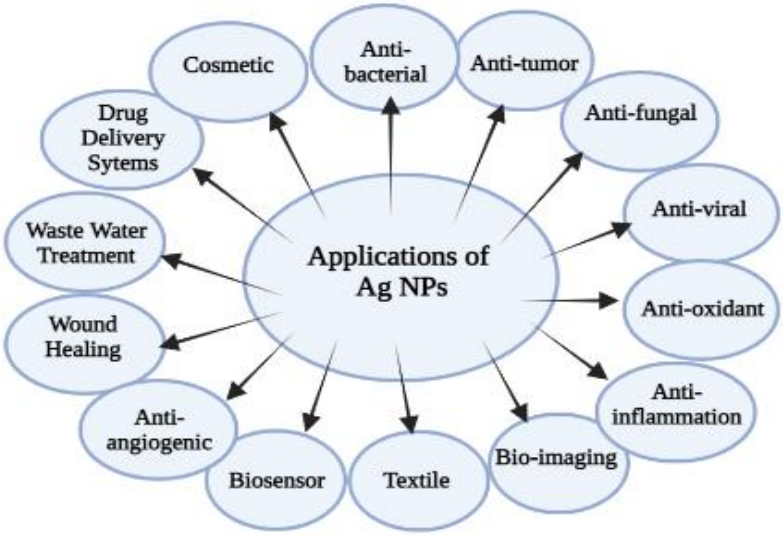

Figure 2.8 Schematic representation of silver nanoparticle usage areas [71]

Silver nanoparticles are one of the silver nitrate derivatives and good antibacterial agents. They can also be incorporated into the wound dressing materials thanks to their numerous physical and chemical characteristics, such as environmental friendliness, low volatility, and excellent thermal stability. These features make AgNPs an effective antibacterial agent [72]. As a result of this, silver NPs are easily preferred in many fields, especially in pharmaceuticals which is shown in Figure 2.8 [71].

AgNPs exhibit an effective antibacterial function due to their significantly large surface area, which enables better contact with the membrane of bacteria. The interaction between AgNPs and bacteria is as follows: The nanoparticles enter within the bacterium and cling to the cell membrane. Then, they interact with sulfur-containing proteins found in the bacterial membrane as well as phosphorus-containing substances like DNA in the cell. After that, AgNPs create a low molecular weight zone in the core of the bacteria and cannot protect itself. As a result of this, membrane permeability is reduced by replacing hydrogen cation, cell division is stopped, and cell death is occurred [67].

2.6.2 Natural Active Components in Wound Dressing

Plant-based approaches continue to play an essential role in primary health care around the world. In recognition of their enormous potential for managing and treating wounds, several plants and their extracts have been employed in traditional and modern medicine. These chemicals possess anti-inflammatory, antimicrobial, and cell-stimulating properties, making them valuable additions to wound healing treatments alongside synthetic active ingredients or even as alternatives to them [68]. In light of their medicinal qualities, cost-effectiveness, and absence of side effects, natural chemicals have been extensively employed in wound healing procedures for thousands of years. These substances induce healing and tissue regeneration through numerous interconnected mechanisms. Natural substances may also be helpful for treating aberrant healing, including keloids and hypertrophic scars. Chrysin, propolis, bromelain, *Calendula officinalis*, *Punica granatum L.* and others are some examples of natural compounds utilized in tissue engineering due to their antibacterial and antioxidant properties [73].

2.6.2.1 Chrysin

In addition to providing antibacterial properties, it is crucial for a dressing material to facilitate an ordered wound healing process. The use of antioxidants in the structure of the dressing material can aid in proper wound healing. Chrysin (5,7-dihydroxyflavone) is a natural polyphenol with antioxidant properties found in honey, propolis, various herbs, and fruits such as bitter melon (*Momordica charantia*) or wild Himalayan pear (*Pyrus pashia*). It has various beneficial effects, such as reducing oxidative stress in the organism, antiviral properties against viruses, ability to alleviate psoriasis-like skin lesions, and anticancer activity that is shown in Figure 2.8. It is believed that incorporating chrysin into the dressing material can help to protect the surrounding tissue from damage caused by bacterial oxidative stress [74].

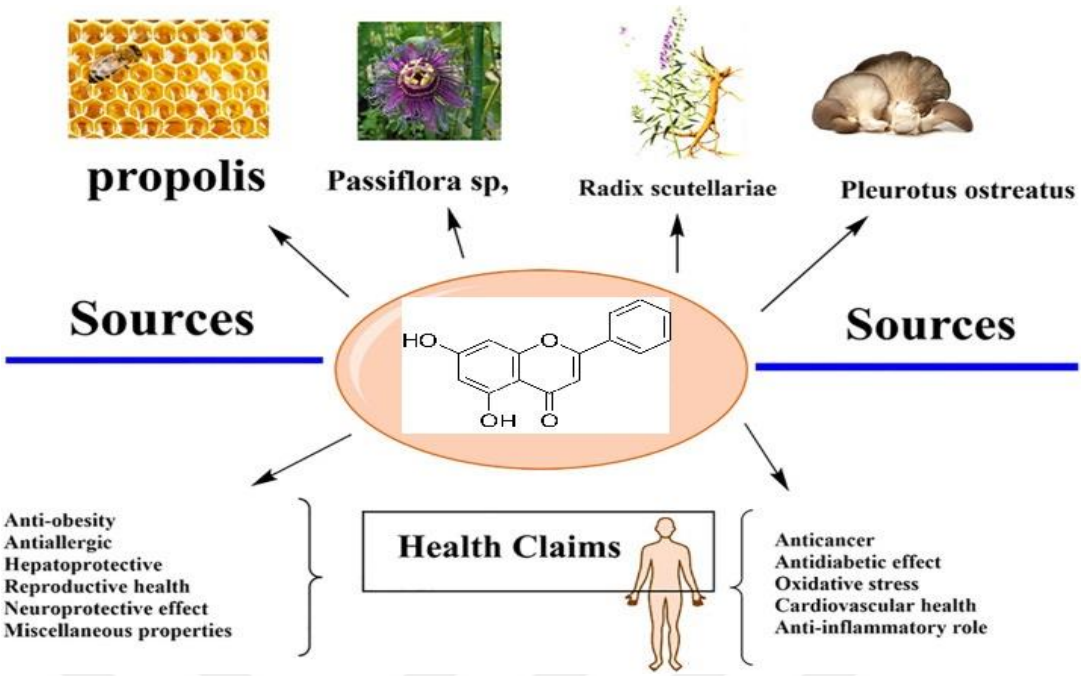

Figure 2.9 Resources and benefits of chrysin [75]

2.7 Wound Dressing Material Production with Electrospinning

There are numerous ways to produce wound treatment products, including 3D printing, chemical dissolution, over-drying into multilayer films, etc. One of these methods is ES, which is a simple technique aimed to produce nanofibrous structures with controlled porosity, diameter, and thickness. In ES, ultrafine nanometric fibers are produced by charging and ejecting a polymer melt or solution via a spinneret under a high-voltage electric field. Then, it is solidified or coagulates to form a filament. This technique is used in different applications such as filters, protective clothes, sensors, energy storages and batteries, catalyst, and especially tissue engineering, scaffolds, and wound dressing due to their characteristic properties such as a high surface area-to-volume ratio, highly interconnected porous architecture, adaptive material properties, as well as ease of adding drugs to NFs during electrospinning which is displayed in Figure 2.9 [76].

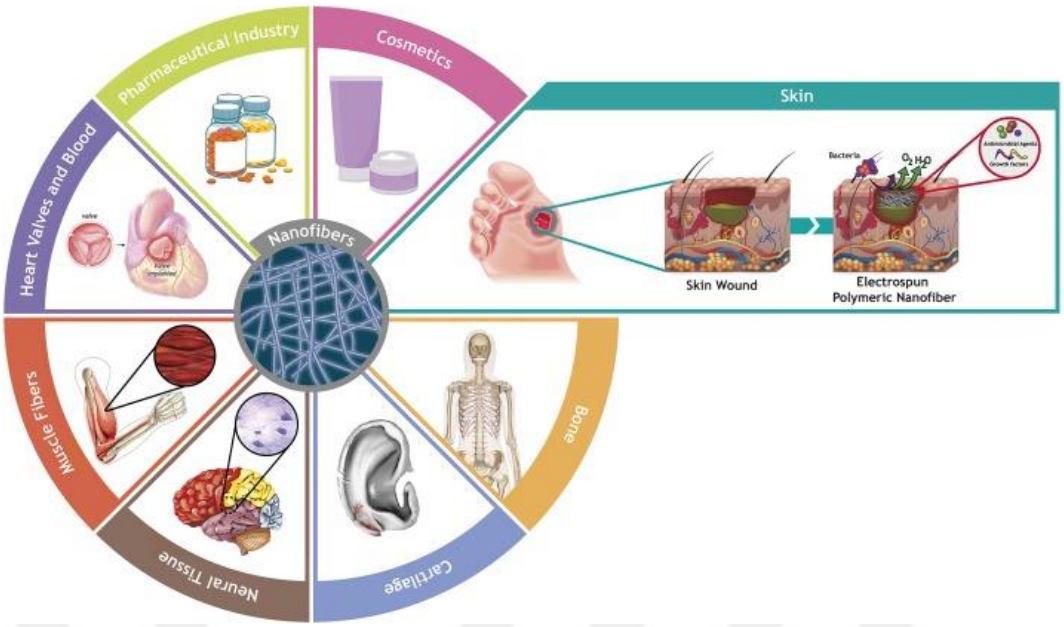

Figure 2.10 The diverse applications of nanofibrous meshes in various biomedical fields [77]

ES involves the utilization of a power supply and electrodes to establish a high-voltage electric field between an injection needle and a collecting surface. As the polymer solution is gradually pushed out of the needle, it forms a hemispherical droplet.

This droplet then elongates into a cone-like shape known as the Taylor cone. Increasing the voltage leads to a gradual rise in the surface charge of the polymer droplet. Once the surface charge reaches a critical point, a polymer jet initiates, accompanied by the vaporization of the solvent within it. This vaporization further increases the surface charge of the jet, causing its destabilization. Consequently, the polymer jet undergoes geometric division, initially splitting into two jets and eventually fragmenting into numerous smaller jets. The formation of nanofiber patterns is facilitated by the electrostatic force, which influences the continuous splitting of polymer droplets [78].

A typical electrospinning system comprises essential components such as a spinneret with a metallic needle, syringe pump, high-voltage power source, and grounded collector which are shown in Figure 2.10. This system enables the production of various polymeric fibers, capitalizing on the processing flexibility offered by electrospinning [79].

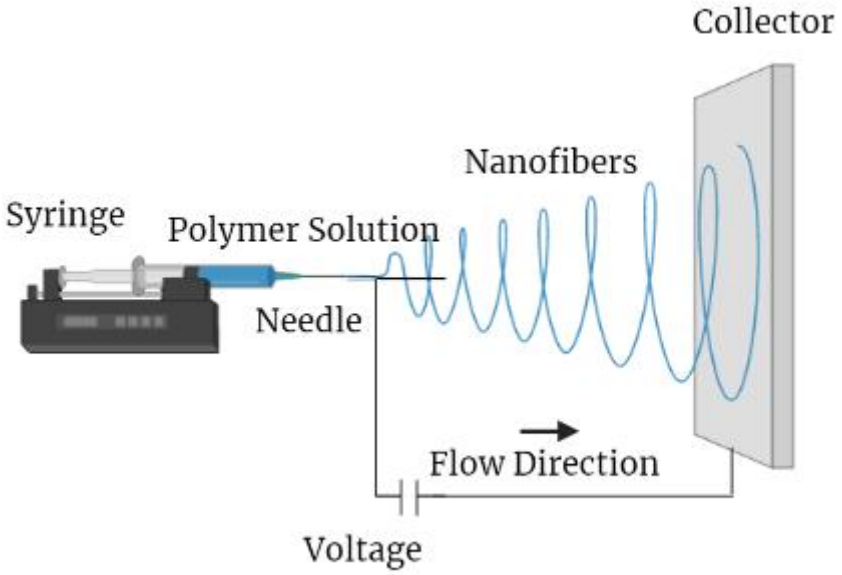

Figure 2.11 Schematic representation of the electrospinning method [80]

There are different types of parameters that affect the ES process, and they are separated into three main categories which are listed in Table 2.2.

Table 2.2 Effecting parameters of the electrospinning process [81]

Electrospinning Parameters		
Solution Parameters	**Processing Parameters**	**Ambient Parameters**
➔ Concentration ➔ Molecular Weight of Polymer ➔ Viscosity ➔ Surface Tension ➔ Conductivity/Surface Charge Density	➔ Voltage ➔ Flow Rate ➔ Collectors ➔ Distance between the Collector and the Tip of the Syringe	➔ Temperature ➔ Humidity ➔ Type Atmosphere ➔ Pressure

All the innate qualities of the solution, manufacturing method, and ambient conditions have an impact on the diameter and shape of electrospun nanofibers.

The shape and final diameter of the electrospun nanofibers are significantly influenced by the inherent properties of the solution, including concentration, viscosity, molecular weight of the polymer, electrical conductivity, elasticity, as well as polarity, and surface tension of the solvent. Optimum solution concentration is necessary to obtain smooth and homogenous nanofibrous biomaterials during electrospinning. Unwanted droplets may occur when low concentration solutions are employed; this could be due to surface tension effects. Additionally, the creation of the fibers would be also difficult at large concentrations due to the high viscosity of the solution. Besides that, the average fiber's diameter decrease may as well as the polymer concentration rises [82].

The key consideration in determining fiber morphology is solution viscosity. Very low viscosity makes it impossible to produce continuous, smooth fibers, whereas very high viscosity causes the hard ejection of jets from the solution, proving the need for an appropriate viscosity for electrospinning. Typically, the concentration of the polymer in the solution can be changed to tune the viscosity, resulting in the production of various products. A separate polymer or oligomer solution has a different range of viscosity that can be used for electrospinning. It is crucial to understand the relationship between viscosity, polymer concentration, and polymer’s molecular weight.

Surface tension is the main cause of the formation of beads or beaded fiber in low viscosity solutions [83]. Many different polymers can be used to successfully generate fibers with diameters ranging from 3 nm to 5 mm. The main purpose of the dressing material is to mimic the fiber structure of the natural surrounding tissue [65]. Since the collagen fibers forming the skin layer are also in fiber structure, it is very advantageous to use the electrospinning method in the production of wound dressing films. So far, electrospinning has been used with many synthetic and natural polymers, including PLGA, PVA, polycaprolactone (PCL), PVDF, polyhydroxybutyrate (PHB), polyethylene glycol (PEG), collagen, silk fibroin, chitosan, gelatin, and hyaluronic acid (HA) [84]–[90].

3
MATERIALS AND METHOD

3.1 Materials

Table 3.1 Materials used in the experiments

Material	Source
4VP	Sigma Aldrich
1-bromohexane	Sigma Aldrich
PLGA (MW=190-240 kg/mol)	Sigma Aldrich
Silver Nitrate ($AgNO_3$),	Sigma Aldrich
Sodium Borohydride ($NaBH_4$)	Sigma Aldrich
Ethyl Alcohol	Sigma Aldrich
Diethyl Ether	Sigma Aldrich
Dimethylformamide (DMF)	Sigma Aldrich
Tetrahydrofuran (THF)	Sigma Aldrich
Dimethyl Sulfoxide (DMSO)	Sigma Aldrich
Trypsin-EDTA (0.25%)	Sigma Aldrich
Chrysin	BLDpharm
Dulbecco's Modified Eagle Medium (DMEM/F12)	Capricorn Scientific
Fetal Bovine Serum (FBS)	Capricorn Scientific
Penicillin-streptomycin	Capricorn Scientific
MTT [3-(4,5-dimethylthiazol-2yl)-2,5-diphenyltetrazolium bromide]	Biomatic
Fibroblast cell (L929)	YTU, Bioengineering Department, Cell Culture Laboratory
PBS (Phosphate Buffer Solution)	Sigma Aldrich
L. Bertani (LB) broth medium	Capricorn Scientific
L. Bertani (LB) agar medium	Capricorn Scientific
Sterile cotton swab	Fischer Scientific
Tryptone	AppliChem
NaCl	Multicell
Agar	Biolife
Yeast extract	AppliChem

3.2 Equipment

Table 3.2 Equipment used in the synthesis and analysis of the samples

Equipment	Brand
Precision Scale	Precisa
Magnetic Stirrer	Heidolph, MR 3000, Germany
Electrospinning Machine	Nanofen Electrospinning System
Laminar Flow Cabin	Faster
Incubator	Binder
Centrifuge	Himac
Shaking Water Bath	N-BIOTEK/GFL
FTIR with ATR attachment	Thermo Scientific / Nicolet iS10
SEM	IEM 11
Ion Sputter Coater	COXEM, SPT-20
Image Investigation Software	Fibraquant
Inverted Microscope	Olympus
Microplate Reader	Multiskan™ FC
Incubator	Memmert
Laminer flow cabin	N-BIOTEK Leading Biotechnology

3.3 Experimental Method

The experimental steps, listed item by item below and also shown in the diagram 3.1, were performed to reach the targeted materials.

1. Synthesis of P4VP
2. Electrospinning of P4VP-PLGA-chrysin nanofiber matrix
3. Reduction of AgNPs on P4VP-PLGA nanofiber matrix

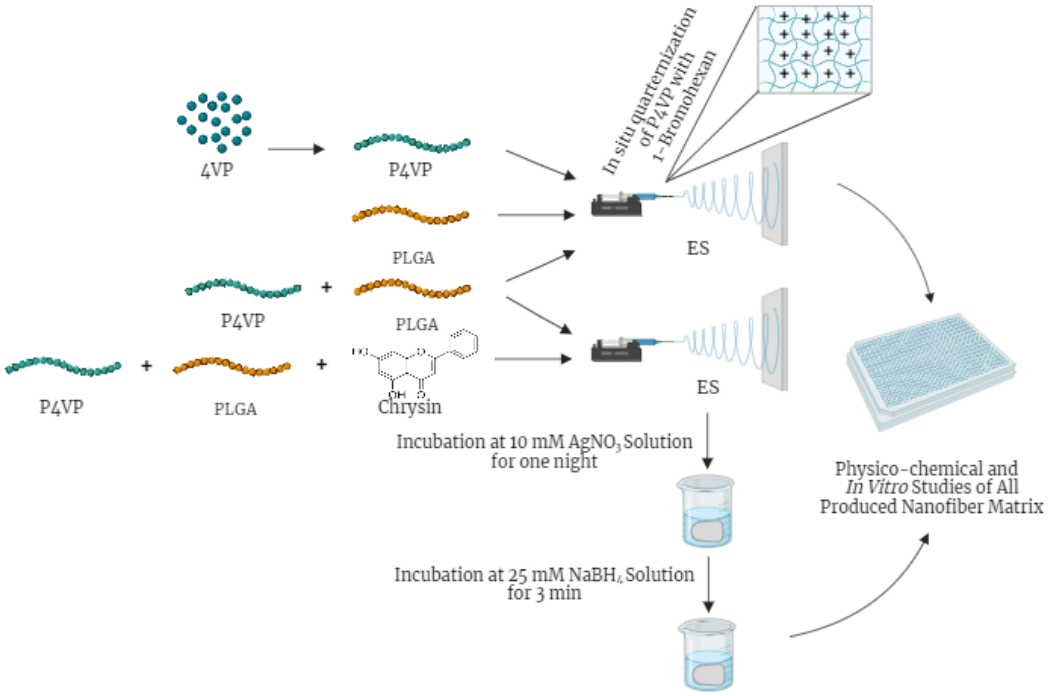

Figure 3.1 Schematic representation of experimental method

3.3.1 Synthesis of P4VP

The cationic polymer of P4VP was synthesized using free radical polymerization which is based on the work of Gokkaya et al. as shown in Figure 3.2 [91]. To begin, 2 M of 4VP was dissolved in DMF and the solution was purged with N_2 gas for 20 minutes to remove dissolved oxygen.. Then, the solution was heated to a temperature of 70°C. The polymerization process was initiated by adding an AIBN (azobisisobutyronitrile) solution to the monomer solution. The initial molar ratio of the monomer to the initiator ($[M]_0/[I]_0$) was 500:1. The free radical polymerization reaction was allowed to proceed for 24 hours.

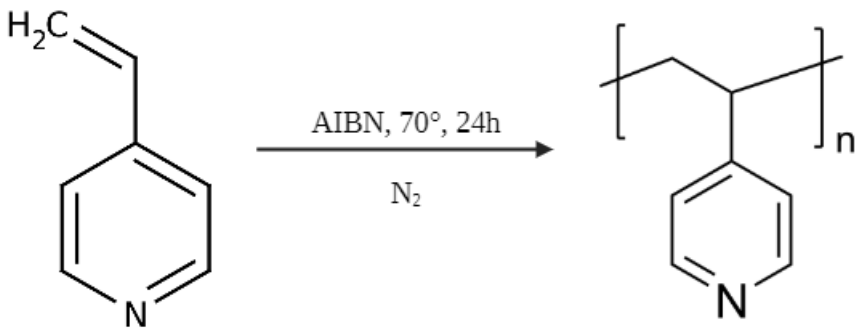

Figure 3.2 Free radical polymerization of poly(4VP)

After the reaction, the polymer formed was precipitated using excess cold diethyl ether. To further purify the polymer, it was dissolved in methanol and then precipitated once again using excess cold diethyl ether.

This additional purification step aimed to remove any remaining unreacted monomers and DMF from the polymer. The final product was vacuum dried for 24 hours at 50°C.

FTIR spectroscopy was used to analyze the chemical structure of the polymer, while the molecular weight (MW) and MW distribution of the polymer were determined using Gel Permeation Chromatography (GPC).

3.3.2 Preparation of P4VP and PLGA Nanofiber Matrix

Electrospinning of P4VP

P4VP based nanofibers were prepared using electrospinning technique. For this purpose, 0.75 g of P4VP was dissolved in 2.5 ml of DMF by stirring at room temperature for 2 hours. After the dissolution of the polymer, 5.5 µl of 1-bromohexane was added to the solution to achieve quaternization of pyridine rings to obtain cationic and inherently antibacterial dressing material. In this ES study, the distance, voltage and feed rate were 10 cm, 18 kV and 0.8 ml/h, respectively.

Electrospinning of PLGA

PLGA based nanofibers were prepared using electrospinning technique. For this purpose, 0.3 g of PLGA was dissolved in 2.5 ml of a 1:1 mixture of DMF and THF by stirring at room temperature for 2 hours. After the preparation solution, PLGA was electrospun to obtain nanofiber matrix. In this ES study, the distance, voltage and feed rate were 10 cm, 18 kV and 0.2 ml/h respectively.

Electrospinning of the mixture of P4VP/PLGA

The solution of P4VP and PLGA was prepared with a total polymer concentration of 15% (w/v). For this purpose, 0.2 g PLGA (85:15) and 0.1 g P4VP were dissolved in a 1:1 mixture of DMF and THF. 5.5 µl of 1-bromohexane was added to this mixture and stirred at room temperature for 2 hours. Thereafter, the electrospinning process was started to obtain the nanofibers from P4VP and PLGA mixture. The distance, voltage and feed rate were 10 cm, 22 kV and 1.0 ml/h, respectively.

Electrospinning of the mixture of P4VP/PLGA/Chrysin

The solution of P4VP, PLGA and Chrysin was prepared with a total polymer concentration of 15% (w/v). For this purpose, 0.2 g PLGA and 0.1 g P4VP were dissolved in a 1:1 mixture of DMF and THF. 5.5 µl of 1-bromohexane and 50 mg of chrysin were added to the solution and stirred at room temperature for 2 hours. Then, the electrospinning process was started to obtain the nanofibers from P4VP and PLGA mixture. The distance, voltage and feed rate were 10 cm, 22 kV and 1.0 ml/h, respectively.

3.3.3 Reduction of AgNPs on Mixed Nanofiber Matrix

After the electrospinning process, silver nanoparticles were introduced into the polymeric nanofiber matrix through the following procedure.

The precursor used in this method was a 10 mM $AgNO_3$ aqueous solution to be reduced for production of the nanoparticles. The binding of silver ions to the fiber surface was achieved through the complexation of silver ions by nanofibers.

The mixed nanofiber matrix was immersed in a 10 mM $AgNO_3$ solution for an entire day. After the incubation process, the nanofiber matrix was washed with water, and then the silver ions were reduced with a 25 mM $NaBH_4$ aqueous solution for three minutes. After reduction of Ag ions, the color of nanofiber matrix turned from white to brown after washing and drying it. The color change is the indicator of the development of Ag nanoparticles which is anchored on the fiber surface.

3.3.4. Characterizations

The chemical structure and functional groups of the polymer and produced materials were investigated using the FTIR spectroscopy. The spectra were acquired with a scanning range of 4000-400 cm^{-1} at a resolution of 4 cm^{-1}.

The Viscotek TDA302 GPC system equipped with refractive index and light scattering detectors was employed to determine the molecular weight and molecular weight distribution of the synthesized P4VP. The separation process utilized an Eprogen CatSEC300 column, with a flow rate of 0.2 ml/min. For the mobile phase, a 0.1 M acetic acid solution containing 0.15 M NaCl was used. Prior to analysis, the samples were filtered through a 0.45 μm syringe filter.

The morphology of the nanofibers was examined using a SEM with an acceleration voltage of 20 kV. Prior to imaging, the samples were cut into suitable sizes and coated with gold and palladium for approximately 120 seconds using an ion sputter coater. The average fiber diameter and distribution were determined using image software of Fibraquant.

The water absorption behavior of the materials were investigated for all the produced nanofiber membranes. Equal-weight samples were immersed in phosphate buffered saline (PBS) with a pH of 7.4, at 37 °C. At various time intervals (3, 6, 9, 12, 15, 20, 25, 45, 60, 75, 90, 120, 150, and 180 minutes), the samples were withdrawn from the PBS solution and weighed. The water absorption ratios (%) were then calculated with the Equation 1. This study was performed in triplicate.

$$\text{Water absorption (\%)} = \frac{\text{Weight of the membrane after incubation (mg)}}{\text{Initial weight of the membrane (mg)}} x100 \qquad (3.1)$$

3.3.5. *In Vitro* Assays

After analyzing the physicochemical characteristics of all produced fiber matrices, in vitro biological assays were conducted to determine the antibacterial activity, biocompatibility, and wound healing characteristics of the produced materials.

3.3.5.1. Investigation of Antibacterial Efficacy of Produced Electrospun Mats

The antibacterial effects of the produced nanofiber mats were examined against gram-negative *Escherichia coli* (*E.coli*) and gram-positive *Staphylococcus aureus* (*S.aureus*) bacteria which were selected as model organisms. The following procedures followed to achieve this goal:

Preparation of medium

For 1 l, 5 g of yeast extract (AppliChem), 10 g of tryptone (AppliChem), 10 g of NaCl (Multicell), and 12 g of agar (Biolife) were added to 1 l of distilled water and stirred. Next, the media was sterilized in an autoclave set at 121°C for 15 minutes. The broth was then rapidly cooled to +4°C. The agar-containing petri dishes were poured, allowing them to reach a near-temperature state, and subsequently, they were covered with parafilm and stored at +4°C [92].

Preparation of samples

Samples cut into 1x1 cm dimensions were sterilized with UV light for 45 minutes before the experiment. The antibacterial properties of the samples were investigated using the disk diffusion method against *S. aureus* and *E. coli* bacteria [93]. The bacteria were cultured in LB broth medium, and their concentrations for the experiment were adjusted to 10^8 CFU/mL using a UV spectrophotometer. Subsequently, the bacterial cultures were evenly spread in three directions on LB agar petri dishes using a swab. The samples were then placed in the center of the bacterial petri dishes using sterile forceps, and the petri dishes were incubated for 24 hours in an oven set at 37°C.

After this incubation period, the diameters of the inhibition zones formed in the petri dishes were measured using a caliper, and images of the petri dishes were captured. The antibacterial activities among the experimental groups were compared based on the zone diameters.

3.3.5.2. Preparation of Cell Cultures

L929 fibroblast cells were used for the analysis of cell viability and in vitro wound healing assays. These cells were cultured in DMEM/F12 growth medium containing 10% FBS and 1% penicillin-streptomycin. The incubator was adjusted to the conditions of 95% humidity, 5% CO_2, and 37°C, and it was used for the experiment [94]. Once the cells reached 70-80% confluency in a 75T flask, they were passaged. During the passaging process, the cell medium was first washed with 1X PBS. Subsequently, the cells were collected in a Falcon tube using 0.25% trypsin-EDTA solution and centrifuged. After centrifugation, the supernatant was discarded, and the remaining cell pellet was suspended in 1 ml of growth medium. Cell counting was performed using a Thoma chamber with trypan blue staining. The required number of cells for the experiments was then suspended in growth medium and used for cell seeding.

3.3.5.3. Biocompatibility Assay

The biocompatibility of the nanofibers was analyzed using the ISO 10993-12 standard extract method (indirect) on L929 fibroblast cells [95].

For this purpose, the fibers were first cut into 2 cm^2 dimensions and then subjected to UV sterilization. Subsequently, sterilized fibers belonging to each experimental group were transferred to separate tubes at a concentration of 2 cm^2/ml in the growth medium. The tubes were then placed in a shaking water bath adjusted to 130 RPM and 37°C for 72 hours. After this period, the growth medium containing the fibers was collected and stored at +4°C for use in cell culture studies.

The effects of fibers on cell viability were analyzed using extract media. The cell viability analysis was conducted using the MTT method. In this method, the tetrazolium component present in the MTT salt is converted to formazan by mitochondrial enzymes in live cells. Thus, the resulting formazan density provides information about cell viability [96].

For the cell viability analysis, fibroblast cells were seeded in 96-well plates with 10^4 cells per well, and the plates were then incubated for 24 hours. After this period, the medium in the wells was aspirated.

The control group wells were replaced with fresh growth medium, while the experimental group wells were replaced with extracts where the fibers had been kept. Each group was tested in triplicate (n=3). Subsequently, the plates were incubated for 24 and 72 hours, and at the end of these periods, the MTT test was performed.

For this test, 10 µl of MTT solution prepared with PBS at a concentration of 10 mg/ml was added to each well, and the plates were incubated in the dark for 4 hours. During this time, live cells converted the yellow tetrazolium compound into purple formazan. Then, to dissolve the insoluble formazan crystals, 100 µl of DMSO solvent was added to each well, and the plates were kept in the dark for 30 minutes. The optical densities (OD) of the formazan crystals in the wells were measured at 570 nm using a microplate reader. The average absorbance values were calculated, and ±SD was determined. Additionally, using the obtained absorbance values, cell viability (%) was calculated with Equation 2.

$$\text{Cell viability (\%)} = \frac{OD_{sample}}{OD_{control}}\ x\ 100 \qquad (3.2)$$

3.3.5.4. *In Vitro* Wound Healing Experiment

The scratch method was used to investigate the effects of fibers on in vitro (2-dimensional environment) wound healing [97]. For this experiment, L929 fibroblast cells were first seeded in a 24-well plate with 10^5 cells per well, and the plates were incubated under appropriate conditions for 24 hours. After this period, the medium in the wells was aspirated, and a 200 µl sterile pipette tip was used to create scratches in the wells. Subsequently, the wells were washed with PBS to remove detached cells from the surface. While fresh growth medium was added to the control group wells, the experimental group wells received extracts of the fibers. Then, the initial states (0 hours) of the scratches in the wells were visualized and recorded using an inverted microscope.

This process was repeated at 24 and 48 hours. The wound areas in the wells of the control and experimental groups were measured using ImageJ software. The obtained data were used in Equation 3 to calculate wound closure (%) in which $G_{(0)}$ is the initial wound area and $G_{(t)}$ is the wound area at t hours after scratching.

$$\text{Wound closure (\%)} = \frac{(G_{(0)}/G_{(t)})}{G_{(0)}} \; x \; 100 \qquad (3.3)$$

4
RESULT AND DISCUSSION

The thesis aims to develop a functional nanofiber-structured wound dressing material to effectively treat common wounds which have the potential to progress into chronic conditions due to various pathogens. For this purpose, the cationic P4VP was synthesized and electrospun together with PLGA and chrysin to form a nanofibrous system. Then, AgNPs were formed on the nanofibers to form the final antibacterial and antioxidant nanofibrous wound dressing material.

Initially, P4VP was synthesized using free radical polymerization. The produced polymer was characterized with FTIR spectroscopy and GPC. Figure 4.1 displays the GPC chromatograms of P4VP obtained from the RI and RALS detectors. The chromatogram exhibits a unimodal peak at 2.4 ml, which corresponds to the polymer. Additionally, small positive and negative peaks observed between 3.4 and 3.9 ml are injection-sourced peaks commonly present in all chromatograms. The GPC analysis yielded a MW of 75 kDa and polydispersity index (PDI) of 1.377 for the P4VP polymer, confirming the successful polymerization.

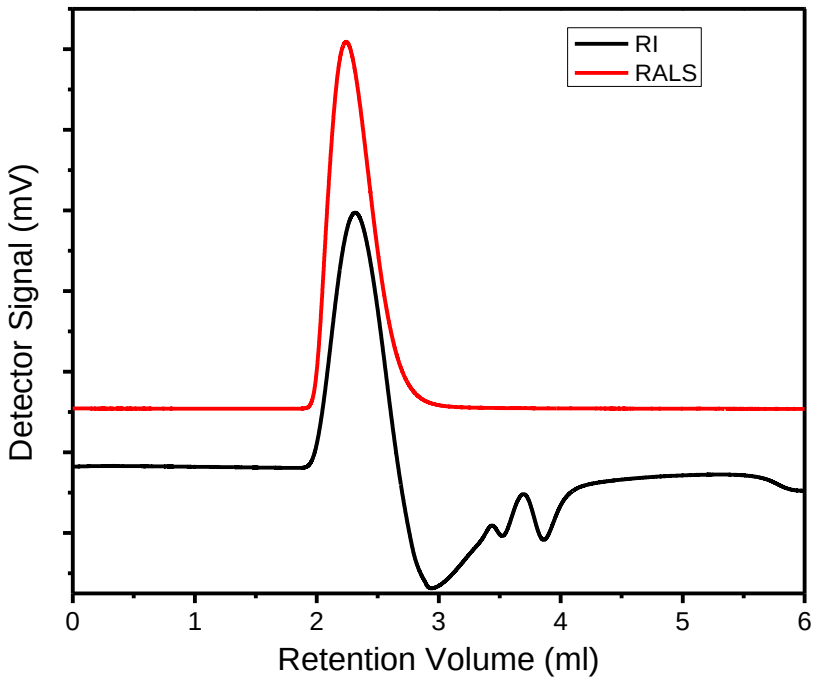

Figure 4.1 GPC chromatograms of P4VP acquired from RI and RALS detectors

After the GPC analysis, the polymer was characterized with FTIR spectroscopy. In Figure 4.2, FTIR spectrum of the synthesized P4VP is given in which the band at 1595.32 cm^{-1} belongs to the pyridine ring stretching. The pyridine is also characterized with the band at 1414.53 cm^{-1}. The band at 3023.35 cm^{-1} belongs to the C-H stretching in aromatic pyridine ring, while the presence of C-H groups in the backbone of the polymer is observed by the band at 2917.23 cm^{-1}. Aromatic C-H groups display out-of-plane deformation vibrations at 819.60 cm^{-1}. It is obvious that aliphatic C-H groups are present in the final product after polymerization which reveals the aliphatic backbone of the polymer, which is absent before the polymerization.

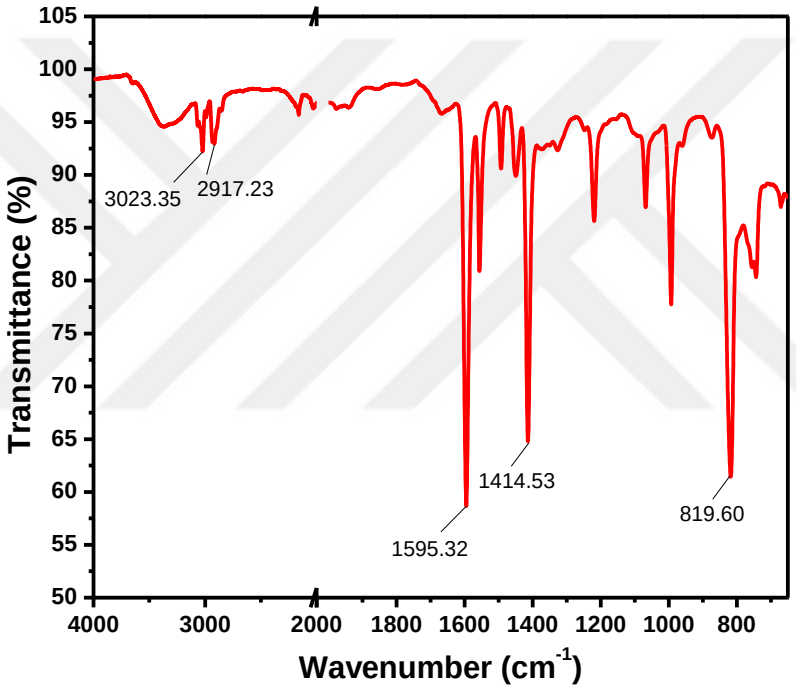

Figure 4.2 FTIR spectrum of synthesized P4VP

The FTIR spectrum and GPC chromatograms clearly exhibits the successful synthesis of P4VP which can be used in the electrospinning of the nanofibers for production of the wound healing materials.

After preparation of P4VP, the nanofiber based wound healing materials are produced using electrospinning technique. For this purpose, different combinations of the components were electrospun to better understand the biological effect of the component.

Figure 4.3 gives the images of nanofiber mats obtained after electrospinning P4VP and PLGA individually and combined together with AgNPs and CHR in different combinations. As seen in Figure 4.3A-B, individual P4VP and PLGA nanofiber matrices obtained on aluminum surface are white colored materials. Electrospinning of the solution of P4VP/PLGA blend also resulted in white-colored material (Figure 4C). The incorporation of AgNPs by reducing Ag ions on the electrospun nanofiber matrix of P4VP/PLGA blend exhibited a brown-colored material (Figure 4D) in which the AgNPs caused the brown color. In the next combination of components, CHR was added to the solution of P4VP/PLGA blend and electrospun to form a white-colored material (Figure 4E). After combining all components together to form a nanofiber matrix from P4VP/PLGA/CHR blend with AgNPs, a light brown-colored material was obtained (Figure 4E) in which the AgNPs presence caused brown color.

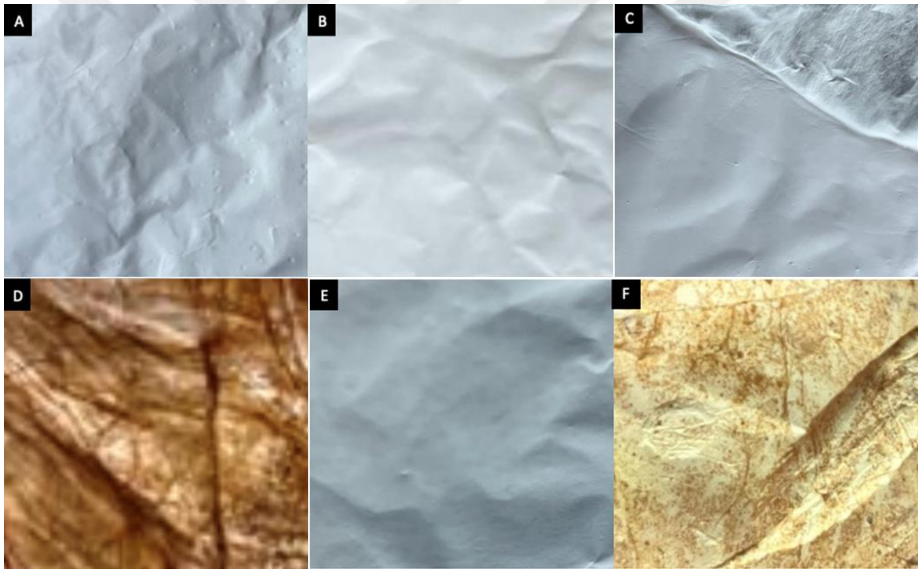

Figure 4.3 Nanofiber matrix pictures of (A) P4VP, (B) PLGA, (C) P4VP/PLGA blend, (D) P4VP/PLGA blend with AgNPs (E) P4VP/PLGA/Chrysin blend and (F) P4VP/PLGA/Chrysin blend with AgNPs

After visually confirming the mat production, SEM was used to prove the nanofiber formations in the produced materials. Figure 4.4 gives the SEM images of all the electrospun materials at 5 kX magnification. SEM images of electrospun materials gives information about the diameter and distribution of the fibers throughout the material.

As seen in all images of Figure 4.4, fibers are formed in all combinations of components and beads were not observed in any of these fibrous materials. However, a few junctions are seen only in the nanofibers produced from individual PLGA (Figure 4.4B).

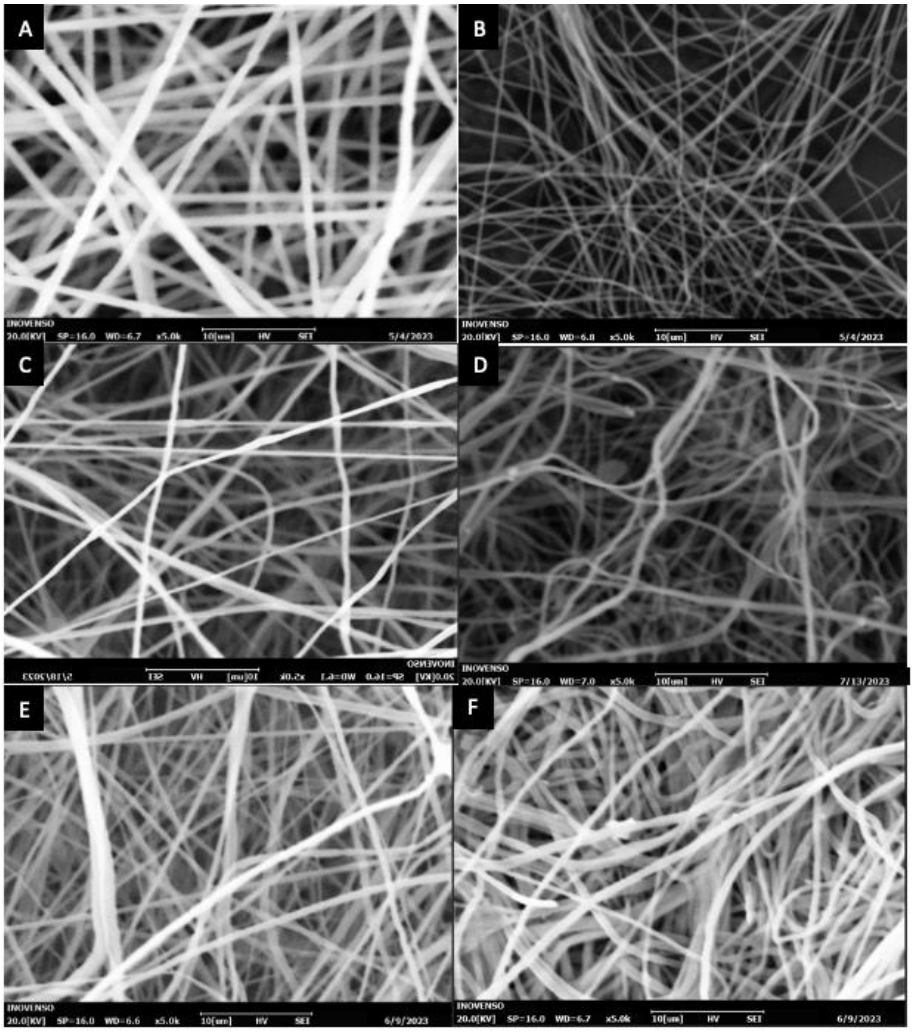

Figure 4.4 SEM images of (A) P4VP, (B) PLGA, (C) P4VP/PLGA blend, (D) P4VP/PLGA blend with AgNPs (E) P4VP/PLGA/Chrysin blend and (F) P4VP/PLGA/Chrysin blend with AgNPs acquired at 5kX magnification

SEM images of the matrices were used to determine the average diameters of the fibers. Table 4.1 gives the average diameters of the fibers produced from all the combinations of components. In the Table 4.1, fibers produced from individual P4VP exhibits the largest diameter as 829 nm, while the fibers obtained by the electrospinning of individual PLGA have the smallest average diameter as 300 nm.

The blend of P4VP and PLGA resulted in an average diameter as 377 nm which is between the diameters of individual P4VP and PLGA. When the AgNPs are incorporated on the nanofibers from P4VP/PLGA blend, the average diameter increased to 392 nm. When the blend of P4VP, PLGA and CHR is electrospun, the produced fibers exhibited the average diameter of 509 nm which reveals that CHR causes in increase in the diameter of nanofibers. The addition of CHR into the polymeric nanofiber matrix has led to an increase in the average fiber diameter. It is thought that chrysin molecules adhered to the fibers during the electrospinning process and affected their dimensions. After incorporation of AgNPs on the nanofibers from P4VP/PLGA/CHR blend, the average diameter increased to 554 nm. The addition of AgNPs to the nanofibrous structure causes an increase in the average diameters and the nanoparticles appear as distinct spots, indicating their presence within the matrix. The fiber diameters obtained in this study are compatible with similar studies such as the study of Gors et al. in which nanofibers with varying concentrations of AgNPs resulted in an average diameter within the range of 67-781 nm [98].

Table 4.1 Average fiber diameters of (A) P4VP, (B) PLGA, (C) P4VP/PLGA blend, (D) P4VP/PLGA blend with AgNPs (E) P4VP/PLGA/Chrysin blend and (F) P4VP/PLGA/Chrysin blend with AgNPs

Sample ID	Fiber Diameter (nm)		
	Average	Std. Dev.	Median
A	829	276	795
B	300	133	258
C	377	160	347
D	392	178	366
E	509	247	475
F	554	237	515

After proving the fiber formations in the produced materials, FTIR spectrometry was used to evaluate their chemical structures. Figure 4.5 depicts the FTIR spectra of the individual and combined samples of P4VP, PLGA, Chrysin, and AgNPs.

When examining the spectra of nanofibers from individual P4VP in Figure 4.5, it can be observed that the bands at 1598, 1558, 1496, and 1417 cm^{-1} in the spectrum attributed to P4VP represent the characteristic vibration peaks of the pyridine ring. Additionally, the peaks at 1068 and 962 cm^{-1} correspond to in-plane and out-of-plane C-H bending vibrations, respectively. In addition, a new band appeared at 1640 cm^{-1} which is different than the only P4VP. This band exhibits the quaternized pyridine ring, which forms by the reaction between 1-bromohexane and nitrogen atom of pyridine ring. The positive charge of the quaternized ammonium group makes the polymer positively charged. It should be noted that not all the pyridine rings are quaternized, since there is still a band at 1598 cm^{-1}. The quaternization of pyridine ring with 1-bromohexane occurs at elevated temperatures as 60-80 °C, but during the electrospinning in situ quaternization reaction has been accomplished, which is a rare example of such reactions.

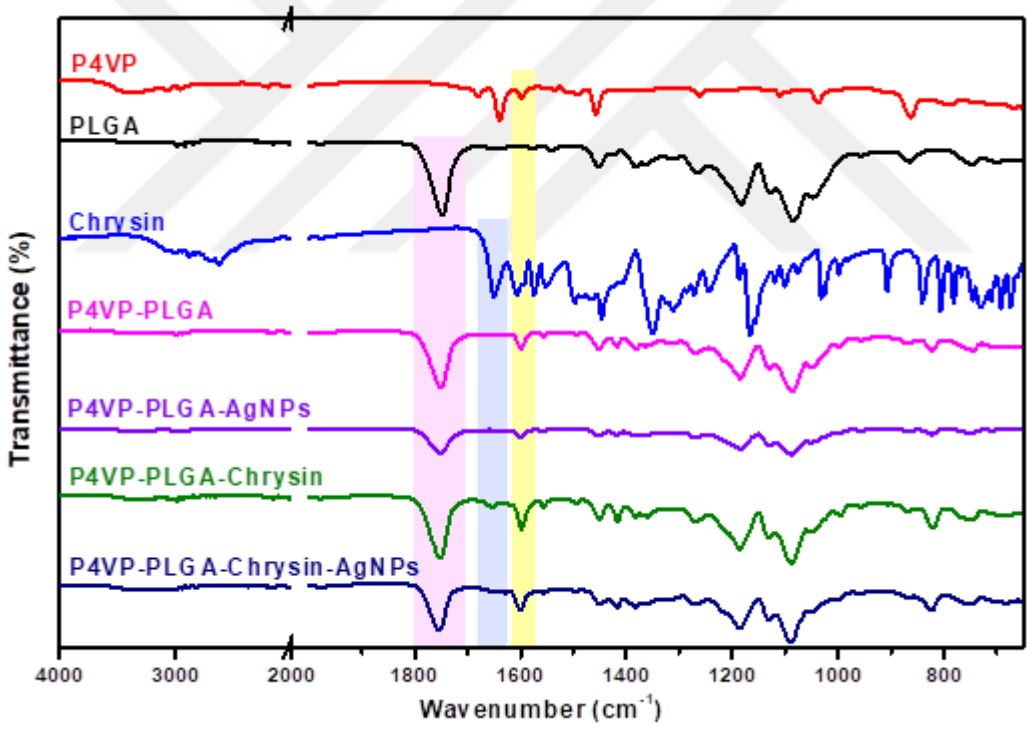

Figure 4.5 FTIR spectra of the produced nanofiber matrices and pure CHR

The spectrum of PLGA nanofibers exhibit bands for carbonyl stretching at 1747 cm^{-1} and for C-O group in the range of 1093–1450 cm^{-1}, indicating the presence of the ester group of PLGA.

The band at 3000 cm^{-1} is attributed to the aliphatic groups of PLGA. These bands provide evidence of the formation of a nanofiber matrix from PLGA. The spectrum of nanofibers from P4VP/PLGA blend in Figure 4.5 demonstrate characteristic bands of both P4VP and PLGA, which provides evidence of the incorporation of both polymers in the nanofiber formation. However, quaternized pyridine rings are not observed in this spectrum. The PLGA chains may have interacted with 1-bromohexane molecules and prevented the quaternization reaction.

CHR molecule is added in the P4VP/PLGA blend solution to electrospun nanofiber matrices. In the pure CHR structure, the bands at 2889 and 2628 cm^{-1} correspond to the stretching vibrations of =C-H and C-H bonds [99]. The carbonyl group vibrations are observed at 1651 cm^{-1} and aromatic ring vibrations are 1606, 1574 and 1446 cm^{-1}. In the nanofibers from P4VP/PLGA/CHR blend, the characteristic bands P4VP, PLGA and CHR were observed at 1597, 1750 and 1651 cm^{-1}, respectively. The spectrum reveals the incorporation of all the components in the nanofibers.

In the spectra of nanofibers from P4VP/PLGA blend with AgNPs and P4VP/PLGA/CHR blend with AgNPs, the bands of P4VP, PLGA and CHR are observed. However, a distinctive band of AgNPs could not be observed in both spectra, which reveals that a further technique is required for chemical characterization of AgNPs [99].

Figure 4.6 illustrates the water absorption ratios of the electrospun nanofiber matrix. In all matrices, the materials absorb water in the first 3-6 minutes and then lose weight until 180 minutes of the experiment. The weight loss of the materials can be the result of dissolution of P4VP in the water or degradation of PLGA. P4VP based nanofiber matrix absorbed the least amount of water, which can be due its high fiber diameter causing smaller pores between fibers and less absorption. The nanofibers produced from PLGA absorbed more water than P4VP based nanofibrous materials. PLGA nanofibers are much smaller than the P4VP nanofibers and PLGA matrix have larger pores between fibers which may have caused more water penetration into the material.

When P4VP and PLGA blend was electrospun, the diameter of the fibers were between the individual P4VP and PLGA fiber diameters, and the water absorption of the P4VP/PLGA blend nanofibers is between the water absorption values of the individual P4VP and PLGA. When AgNPs were added to the nanofiber matrix of P4VP/PLGA blend, the water absorption reached to a maximum value, which can be the result of increase in the interaction between nanoparticles and water. It was also shown in the study of Liu et al. that AgNPs addition to the nanofibers increased the swelling capacity of nanofiber structures [100]. However, CHR addition to the structure of P4VP/LGA blend with AGNPs slightly decreased the water absorption.

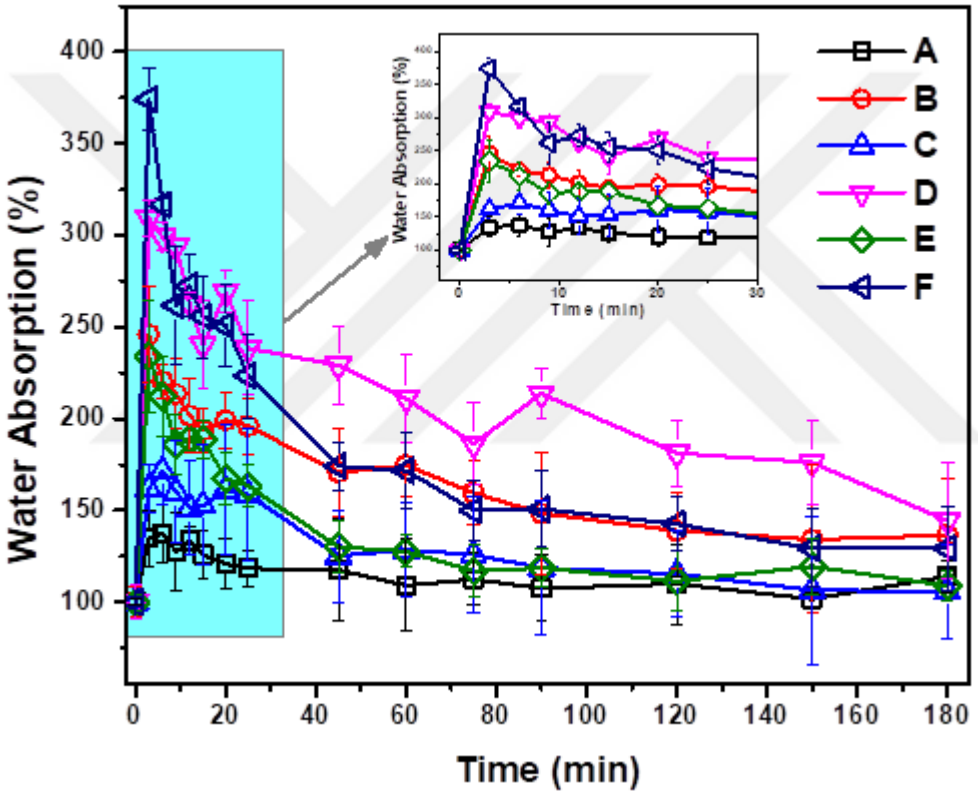

Figure 4.6 Water absorption ratios of (A) P4VP, (B) PLGA, (C) P4VP/PLGA blend, (D) P4VP/PLGA blend with AgNPs (E) P4VP/PLGA/Chrysin blend and (F) P4VP/PLGA/Chrysin blend with AgNPs

After production and characterization of the electrospun mats, their biological activities were evaluated. Firstly, antibacterial activity of the materials were determined against *S. aureus* and *E. coli*.

Secondly, biocompatibility of the electrospun mats were investigated on L929 cells and finally, wound healing efficacy of the produced materials were determined via scratch test.

Table 4.2 shows the petri images of all the samples after incubated with *E. coli* and *S. aureus*. As seen in the Table 4.2, P4VP mats exhibited antibacterial activity only against *S. aureus*. The activity of P4VP is caused by the positive charges on the polymer backbone, which allows the polymer interact with the negatively charged bacterial membrane and disrupt the cell. However, P4VP did not exhibit activity against *E. coli*.

PLGA is a biocompatible and biodegradable copolymer and showed antibacterial activity against both bacteria. This polymer also exhibited a slight antibacterial activity in the study of Liao et al. [101]. The antibacterial activity of the polymer can be attributed to the acidic degradation products of the polymer.

When P4VP and PLGA combined together, the formed electrospun mat exhibited antibacterial activity against both bacteria. Adding AgNPs to the P4VP/PLGA blend mat increased the antibacterial activity considerably, which is caused by the antibacterial efficacy of the AgNPs and diffusion of Ag ions.

CHR addition to the P4VP/PLGA blend mats did not prevent antibacterial activity and the electrospun mats were still active against both bacteria. CHR and AgNPs incorporated P4VP/PLGA mats exhibited a high antibacterial activity against both bacteria.

Table 4.2 Images of agar plates of all the produced samples showing bacterial inhibition zones against *E. coli* and *S. aureus*

Sample	**Microorganism**	
	E. coli	***S. aureus***
P4VP		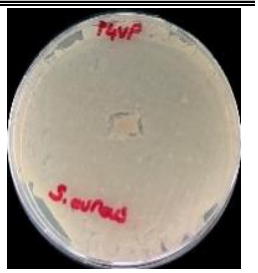

Table 4.3 Images of agar plates of all the produced samples showing bacterial inhibition zones against *E. coli* and *S. aureus* (continued)

PLGA		
P4VP+PLGA		
P4VP+PLGA+AgNPs		
P4VP+PLGA+CHR		
P4VP+PLGA+CHR+AgNPs		

Figure 4.7 gives the inhibition zone values of the samples acquired from the disc diffusion assays against *S. aureus* and *E. coli*. As seen, AgNPs incorporation into the P4VP/PLGA blend nanofiber considerably increased the antibacterial activity of the material. However, when CHR is added to P4VP/PLGA blend nanofiber, a slight increase in antibacterial activity was observed. When both CHR and AgNPs are added to the P4VP/PLGA blend nanofiber, the resulting antibacterial activity was slightly less than P4VP/PLGA blend nanofiber with only AgNPs.

It is obvious that CHR interacts with AgNPs and causes a decrease in the total antibacterial activity. It can be said that the produced nanofibers containing CHR and/or AgNPs are antibacterial materials that are effective against both *S. aureus* and *E. coli*.

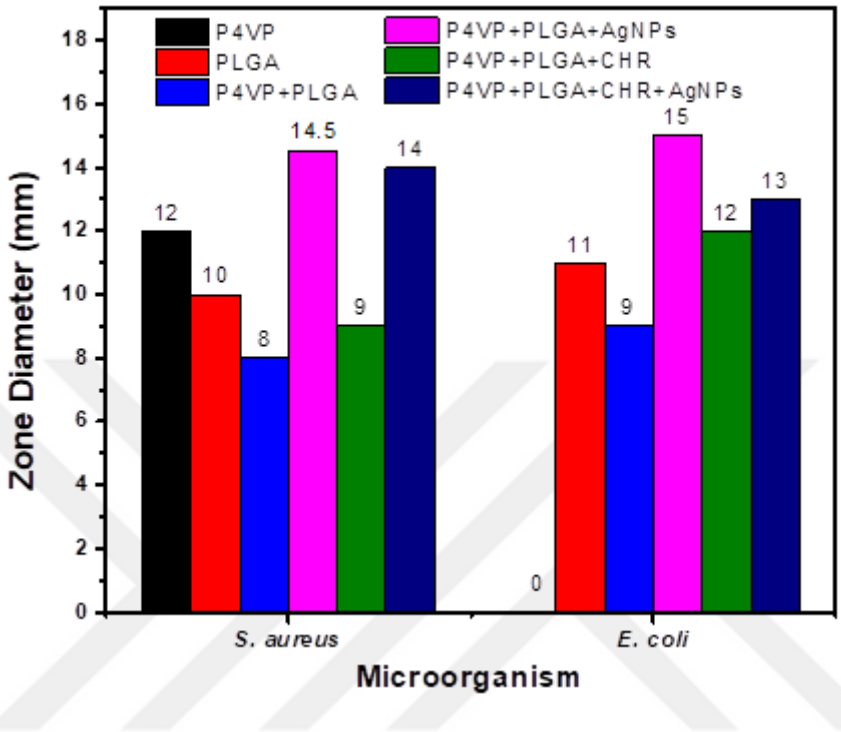

Figure 4.7 Inhibition zone diameter of the electrospun samples against *S. aureus* and *E. coli* acquired from disc diffusion assays

The introduction of a secondary active compound into the nanofiber matrix has led to an increase in antibacterial efficiency. The effect of AgNPs is significantly greater than that of CHR. Consequently, it can be inferred that the increased antibacterial activity results are directly attributed to the presence of AgNPs. Upon comparing the results with the existing studies, researchers also observed that AgNPs have the potential to reduce biofilm formation, and their inhibition zones varied between 7.7 mm and 24 mm depending on the types of bacteria [102]. Thus, the obtained results align with those reported by previous researchers [16].

The biocompatibility of the electrospun materials were evaluated using an indirect method by incubating the extracts of the samples with L929 fibroblast cells. Figure 4.8 shows the cell viabilities after 24 and 48 h incubation of samples' extracts with the L929 cells.

After 24 hours of incubation, all the electrospun matrices were biocompatible on L929 cells. Moreover, the cell viabilities of all samples were higher than the control sample, which indicates that the electrospun materials increase the proliferation of the cells in the first 24 h. After 72 hours incubation of the samples with the cells, cell viabilities decreased to values lower than the control sample. However, the samples that do not contain CHR caused approximately 80% viability of the cell, which can be accepted as biocompatible. The samples containing CHR were toxic after 72 hours of incubation with cells. It was also demonstrated that an elevated concentration of CHR is toxic to human breast adenocarcinoma cells, particularly after 48 and 72 hours, surpassing critical thresholds [103].

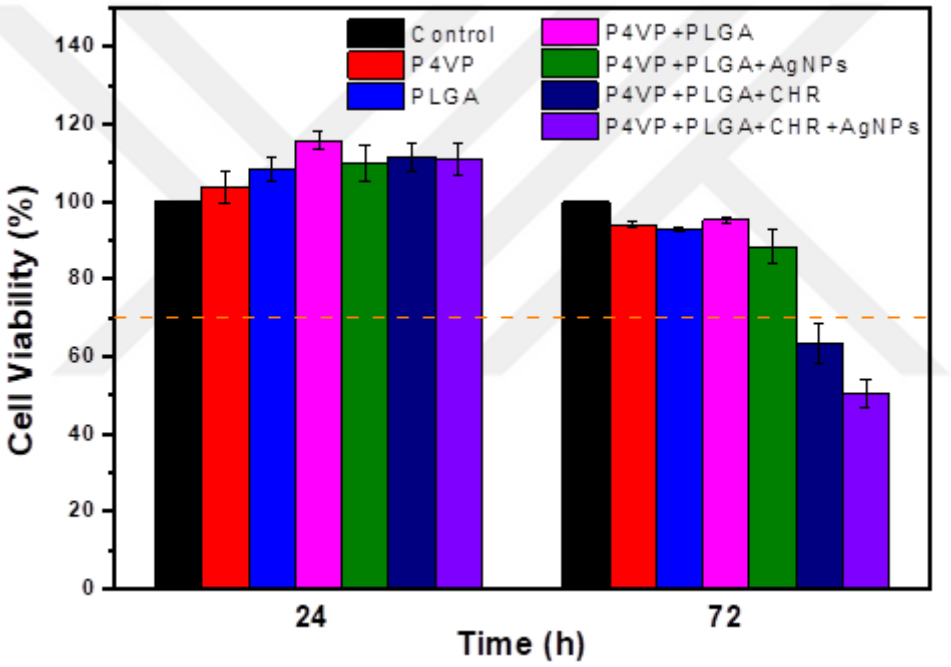

Figure 4.8 The effect of the produced electrospun samples on the viabilities of L929 cells after 24 and 72 h incubation

After evaluating the biocompatibility of the samples, their effect on wound healing was evaluated in vitro using a scratch test. In this test, cells are separated via a scratch and the material is applied to this scratched area to observe any effect in the proliferation of cells in this area. Table 4.3 gives the microscope images of the scratched cell colonies after 24 and 48 hours of incubation with the electrospun samples.

Table 4.4 Invert microscope images (10x) of L929 fibroblast cells after scratched and incubated with the extracts of the samples at different time intervals

Sample	Time (h)		
	0	24	48
Control	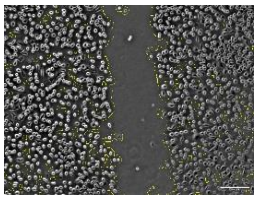	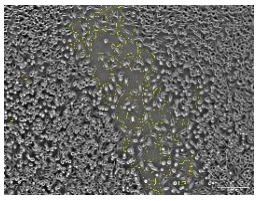	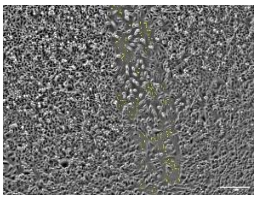
P4VP	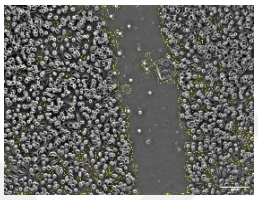	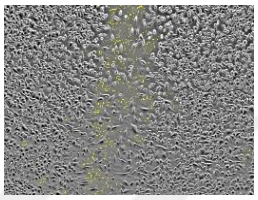	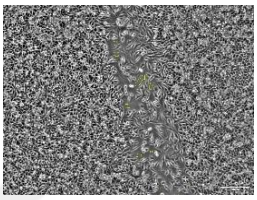
PLGA	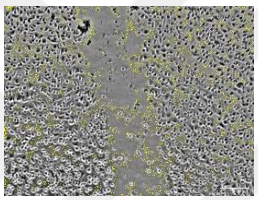	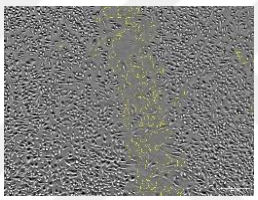	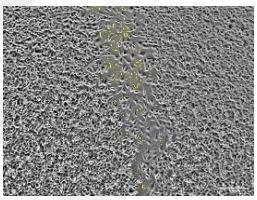
P4VP-PLGA	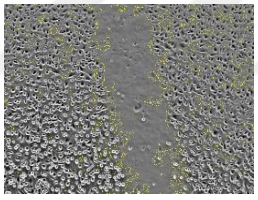	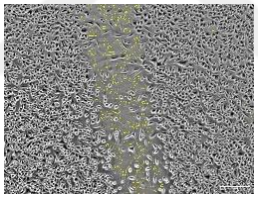	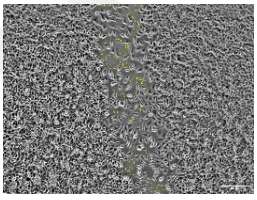
P4VP-PLGA-AgNPs	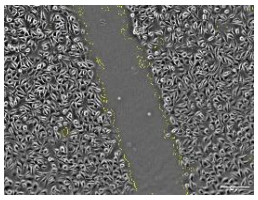	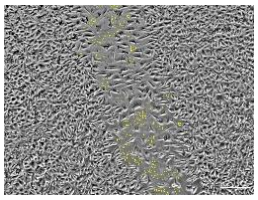	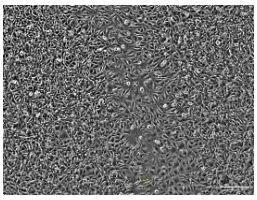
P4VP-PLGA-CHR	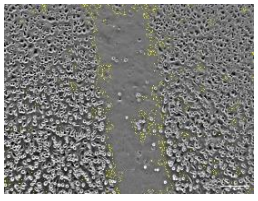	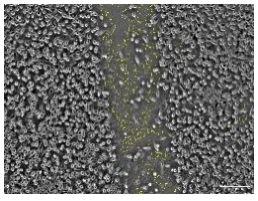	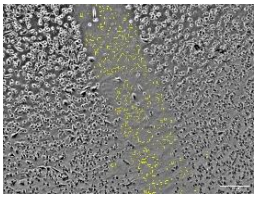
P4VP-PLGA-CHR-AgNPs	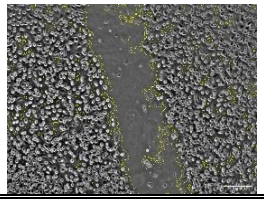	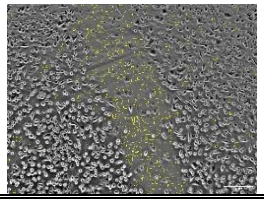	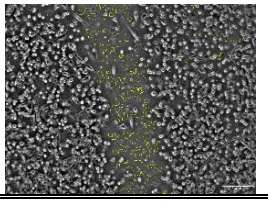

The area of the scratched regions given in Table 4.3 is measured by the image software to evaluate the cell proliferation to cover the scratched area. The obtained areas are proportioned to the initial scratched area and the wound healing ratio percentage is determined. Table 4.4 gives the wound healing values of the samples after applied to the scratched areas in vitro. P4VP increases the wound healing after both 24 and 48 hours compared to the control, which can be attributed to the positive charges of the polymer to increase interaction with the cells. On the other hand, PLGA based nanofibers decreased the wound healing after 24 hours but increased the wound heling after 48 hours. The electrospun matrix composed of a blend of these polymers was also effective in wound healing, inducing accelerated wound healing after both 24 and 48 hours.

AgNPs incorporation onto the P4VP/PLGA blend nanofibers caused a considerable positive effect on wound healing, in which the scratched are almost completely healed after 48 hours. It was shown that AgNPs inhibit the production of proinflammatory cytokines and cause the down-regulation of proinflammatory cytokines leading to earlier wound healing [104]. Therefore, our results are compatible with the previous studies.

CHR incorporation caused a negative effect in the wound healing process. Only after 24 h of incubation with the nanofibers from P4VP/PLGA/CHR caused a slightly positive effect on the wound healing. After 48 hours of incubation with the nanofibers from P4VP/PLGA/CHR decreased the cell proliferation. The nanofibers of P4VP/PLGA/CHR with AgNPs decreased the wound healing compared to the control after both 24 and 48 hours. The negative effect of CHR on the wound healing process can be the result of toxicity of the CHR molecule that inhibits the proliferation of the cells.

Table 4.5 In vitro percentages of wound healing on L929 fibroblast cells after incubation with the electrospun samples

Sample	Wound Healing (%)	
	after 24 h	after 48 h
Control	62.47	90.09
P4VP	77.83	98.22
PLGA	57.80	92.30
P4VP-PLGA	74.92	93.10
P4VP-PLGA-AgNPs	83.37	99.87
P4VP-PLGA-CHR	69.89	71.82
P4VP-PLGA-CHR-AgNPs	55.80	75.13

5
CONCLUSION

The thesis introduces a novel approach by combining antioxidants and silver nanoparticles within a P4VP and PLGA based polymeric electrospun material, which can be used as a wound dressing material. As a result of the findings, the following conclusions can be drawn:

- P4VP polymer was produced and the results acquired from FTIR spectroscopy and GPC revealed that P4VP with 75 kDa MW and its PDI value was 1.377. Thus, unimodal distribution was successfully synthesized.
- P4VP and PLGA were used to prepare electrospun nanofiber matrices in different combinations with AgNPs and CHR. The SEM images showed that nanofibers ranging between 300-829 nm were produced without beads and junctions. It was revealed that as the PLGA content increases, the average diameter of the matrix decreases.
- The white colored nanofiber materials soaked in $AgNO_3$ and then $NaBH_4$, turned the color of material to brown after the treatment, which proves the successful silver reduction on the dressing material surface. Also, the average diameters of nanofibers were larger after treatment with silver, which also indicates the AgNPs formation on the nanofibers.
- The produced nanofibers absorbed water up to maximum 375% depending on the material's composition. It was shown that when AgNPs were added to the nanofiber matrix of P4VP/PLGA blend, the water absorption reached to a maximum value.
- All the produced nanofibers exhibited antibacterial activity against *E. coli* and *S. aureus*, in which the only exception was the P4VP based nanofibers showing activity only against *S. aureus*. The antibacterial activity of the PLGA-based nanofiber matrix is attributed to its biodegradability. During the experiment, the fibers underwent biodegradation and experienced shrinkage.

Subsequently, this process led to the formation of inhibition zones. The addition of AgNPs into the nanofiber structure considerable increased the antibacterial efficacy of the nanofibers.

- In the first 24 hours incubation of L929 cells with the produced materials, all the samples were biocompatible on the studied cell line. However, after 72 hours of incubation, CHR containing nanofibers exhibited toxicity on the cells.
- AgNPs containing nanofibers showed the highest wound healing effect while addition of CHR caused a considerable decrease in the wound healing capacity of the produced nanofiber-based materials.

In conclusion, the produced P4VP-PLGA based nanofiber-based materials have the potential to be used as antibacterial wound healing materials. Incorporation of AgNPs into the structure considerably increased the antibacterial efficacy and wound healing capacity of the material, which indicates the importance of composite production.

In the further studies, silver existence in the material should be characterized in advanced techniques such as XRF (X-ray fluorescence) to better understand the formed structure. Also, change in the concentration of AgNPs and CHR in the nanofiber matrices should be investigated comprehensively to exhibit their combined activity both in antibacterial and wound healing studies.

REFERENCES

[1] E. M. Tottoli, R. Dorati, I. Genta, E. Chiesa, S. Pisani, and B. Conti, "Skin wound healing process and new emerging technologies for skin wound care and regeneration," *Pharmaceutics*, vol. 12, no. 8. MDPI AG, pp. 1–30, Aug. 01, 2020. doi: 10.3390/pharmaceutics12080735.

[2] L. Cañedo-Dorantes and M. Cañedo-Ayala, "Skin acute wound healing: A comprehensive review," *International Journal of Inflammation*, vol. 2019. Hindawi Limited, 2019. doi: 10.1155/2019/3706315.

[3] M. Naseri-Nosar and Z. M. Ziora, "Wound dressings from naturally-occurring polymers: A review on homopolysaccharide-based composites," *Carbohydrate Polymers*, vol. 189. Elsevier Ltd, pp. 379–398, Jun. 01, 2018. doi: 10.1016/j.carbpol.2018.02.003.

[4] D. Simões, S. P. Miguel, M. P. Ribeiro, P. Coutinho, A. G. Mendonça, and I. J. Correia, "Recent advances on antimicrobial wound dressing: A review," *European Journal of Pharmaceutics and Biopharmaceutics*, vol. 127. Elsevier B.V., pp. 130–141, Jun. 01, 2018. doi: 10.1016/j.ejpb.2018.02.022.

[5] M. Mir *et al.*, "Synthetic polymeric biomaterials for wound healing: a review," *Progress in Biomaterials*, vol. 7, no. 1. SpringerOpen, Mar. 01, 2018. doi: 10.1007/s40204-018-0083-4.

[6] A. Alshhab and E. Yilmaz, "Sodium alginate/poly(4-vinylpyridine) polyelectrolyte multilayer films: Preparation, characterization and ciprofloxacin HCl release," *Int J Biol Macromol*, vol. 147, pp. 809–820, Mar. 2020, doi: 10.1016/j.ijbiomac.2019.10.058.

[7] A. BAL ÖZTÜRK and Z. P. AKGÜNER, "İpek Fibroin/Polivinil Alkol Esaslı İlaç Taşıyıcı Yara Örtüleri," *Süleyman Demirel Üniversitesi Fen Bilimleri Enstitüsü Dergisi*, pp. 25–34, Apr. 2020, doi: 10.19113/sdufenbed.561177.

[8] N. Vázquez *et al.*, "Influence of the PLGA/gelatin ratio on the physical, chemical and biological properties of electrospun scaffolds for wound

dressings," *Biomedical Materials (Bristol)*, vol. 14, no. 4, May 2019, doi: 10.1088/1748-605X/ab1741.

[9] I. N. Amirrah, M. F. M. Razip Wee, Y. Tabata, R. B. H. Idrus, A. Nordin, and M. B. Fauzi, "Antibacterial-integrated collagen wound dressing for diabetes-related foot ulcers: An evidence-based review of clinical studies," *Polymers*, vol. 12, no. 9. MDPI AG, Sep. 01, 2020. doi: 10.3390/POLYM12092168.

[10] S. J. Liu, Y. C. Kau, C. Y. Chou, J. K. Chen, R. C. Wu, and W. L. Yeh, "Electrospun PLGA/collagen nanofibrous membrane as early-stage wound dressing," *J Memb Sci*, vol. 355, no. 1–2, pp. 53–59, Jun. 2010, doi: 10.1016/j.memsci.2010.03.012.

[11] E. Watson, A. M. Tatara, D. P. Kontoyiannis, and A. G. Mikos, "Inherently Antimicrobial Biodegradable Polymers in Tissue Engineering," *ACS Biomaterials Science and Engineering*, vol. 3, no. 7. American Chemical Society, pp. 1207–1220, Jul. 10, 2017. doi: 10.1021/acsbiomaterials.6b00501.

[12] M. Yin, S. Wan, X. Ren, and C. C. Chu, "Development of Inherently Antibacterial, Biodegradable, and Biologically Active Chitosan/Pseudo-Protein Hybrid Hydrogels as Biofunctional Wound Dressings," *ACS Appl Mater Interfaces*, vol. 13, no. 12, pp. 14688–14699, Mar. 2021, doi: 10.1021/acsami.0c21680.

[13] E. Kenawy, A. M. Omer, T. M. Tamer, M. A. Elmeligy, and M. S. M. Eldin, "Fabrication of biodegradable gelatin/chitosan/cinnamaldehyde crosslinked membranes for antibacterial wound dressing applications," *Int J Biol Macromol*, vol. 139, pp. 440–448, Oct. 2019, doi: 10.1016/j.ijbiomac.2019.07.191.

[14] X. Li, C. Wang, S. Yang, P. Liu, and B. Zhang, "Electrospun PCL/mupirocin and chitosan/ lidocaine hydrochloride multifunctional double layer nanofibrous scaffolds for wound dressing applications," *Int J Nanomedicine*, vol. 13, pp. 5287–5299, 2018, doi: 10.2147/IJN.S177256.

[15] A. ur R. Khan *et al.*, “Exploration of the antibacterial and wound healing potential of a PLGA/silk fibroin based electrospun membrane loaded with zinc oxide nanoparticles,” *J Mater Chem B*, vol. 9, no. 5, pp. 1452–1465, Feb. 2021, doi: 10.1039/d0tb02822c.

[16] A. Hamad, K. S. Khashan, and A. Hadi, “Silver Nanoparticles and Silver Ions as Potential Antibacterial Agents,” *Journal of Inorganic and Organometallic Polymers and Materials*, vol. 30, no. 12. Springer, pp. 4811–4828, Dec. 01, 2020. doi: 10.1007/s10904-020-01744-x.

[17] S. J. Yu, Y. G. Yin, and J. F. Liu, “Silver nanoparticles in the environment,” *Environmental Sciences: Processes and Impacts*, vol. 15, no. 1. pp. 78–92, 2013. doi: 10.1039/c2em30595j.

[18] K. Kalantari *et al.*, “Wound dressings functionalized with silver nanoparticles: Promises and pitfalls,” *Nanoscale*, vol. 12, no. 4. Royal Society of Chemistry, pp. 2268–2291, Jan. 28, 2020. doi: 10.1039/c9nr08234d.

[19] G. Dai, S. Tang, and T. Wang, “A novel approach to prepare high antibacterial polylactic acid surface encapsulated nano-silver through stereocomplexation,” *Mater Res Express*, vol. 6, no. 5, 2019, doi: 10.1088/2053-1591/ab0330.

[20] Z. Mohammadi *et al.*, “The effect of chrysin–curcumin-loaded nanofibres on the wound-healing process in male rats,” *Artif Cells Nanomed Biotechnol*, vol. 47, no. 1, pp. 1642–1652, Dec. 2019, doi: 10.1080/21691401.2019.1594855.

[21] Y. Deldar, Y. Pilehvar-Soltanahmadi, M. Dadashpour, S. Montazer Saheb, M. Rahmati-Yamchi, and N. Zarghami, “An in vitro examination of the antioxidant, cytoprotective and anti-inflammatory properties of chrysin-loaded nanofibrous mats for potential wound healing applications,” *Artif Cells Nanomed Biotechnol*, vol. 46, no. 4, pp. 706–716, May 2018, doi: 10.1080/21691401.2017.1337022.

[22] G. Sandri, S. Rossi, M. C. Bonferoni, C. Caramella, and F. Ferrari, “Electrospinning Technologies in Wound Dressing Applications,” 2020.

[23] M. T. Sultan, O. J. Lee, S. H. Kim, H. W. Ju, and C. H. Park, “Silk Fibroin in Wound Healing Process,” in *Advances in Experimental Medicine and Biology*, Springer New York LLC, 2018, pp. 115–126. doi: 10.1007/978-981-13-0947-2_7.

[24] J. M. Abdo, N. A. Sopko, and S. M. Milner, “The applied anatomy of human skin: A model for regeneration,” *Wound Medicine*, vol. 28. Elsevier GmbH, Mar. 01, 2020. doi: 10.1016/j.wndm.2020.100179.

[25] J. Kanitakis, “John Libbey Eurotext - European Journal of Dermatology - Anatomy, histology and immunohistochemistry of normal human skin,” 2001. [Online]. Available: https://www.researchgate.net/publication/11279803

[26] E. Hofmann, A. Schwarz, J. Fink, L.-P. Kamolz, and P. Kotzbeck, “Modelling the Complexity of Human Skin In Vitro,” *Biomedicines*, vol. 11, no. 3, p. 794, Mar. 2023, doi: 10.3390/biomedicines11030794.

[27] B. S. Kim, G. Gao, J. Y. Kim, and D. W. Cho, “3D Cell Printing of Perfusable Vascularized Human Skin Equivalent Composed of Epidermis, Dermis, and Hypodermis for Better Structural Recapitulation of Native Skin,” *Adv Healthc Mater*, vol. 8, no. 7, Apr. 2019, doi: 10.1002/adhm.201801019.

[28] S. Supe and P. Takudage, “Methods for evaluating penetration of drug into the skin: A review,” *Skin Research and Technology*, vol. 27, no. 3. John Wiley and Sons Inc, pp. 299–308, May 01, 2021. doi: 10.1111/srt.12968.

[29] C. Hwa, E. A. Bauer, D. E. Cohen, and T. O. Ronald Perelman, “Skin biologyd th_1460 464..470,” 2012.

[30] Y. Liang, J. He, and B. Guo, “Functional Hydrogels as Wound Dressing to Enhance Wound Healing,” *ACS Nano*, vol. 15, no. 8. American Chemical Society, pp. 12687–12722, Aug. 24, 2021. doi: 10.1021/acsnano.1c04206.

[31] G. Broughton, J. E. Janis, and C. E. Attinger, “A brief history of wound care,” *Plastic and Reconstructive Surgery*, vol. 117, no. 7 SUPPL. Jun. 2006. doi: 10.1097/01.prs.0000225429.76355.dd.

[32] Community Health Network, “Types of Wounds,” *https://mychn.org/wound-care-2/*, 2021.

[33] Flen Health, “Acute and Chronic Wounds,” *https://www.flenhealth.com/patients/disease-awareness/acute-chronic-wounds*, 2023.

[34] M. Abazari, A. Ghaffari, H. Rashidzadeh, S. M. Badeleh, and Y. Maleki, “A Systematic Review on Classification, Identification, and Healing Process of Burn Wound Healing,” *International Journal of Lower Extremity Wounds*, vol. 21, no. 1. SAGE Publications Inc., pp. 18–30, Mar. 01, 2022. doi: 10.1177/1534734620924857.

[35] Y. Jiang, X. Xu, L. Xiao, L. Wang, and S. Qiang, “The Role of microRNA in the Inflammatory Response of Wound Healing,” *Frontiers in Immunology*, vol. 13. Frontiers Media S.A., Mar. 21, 2022. doi: 10.3389/fimmu.2022.852419.

[36] S. Barrientos, H. Brem, O. Stojadinovic, and M. Tomic-Canic, “Clinical application of growth factors and cytokines in wound healing,” *Wound Repair and Regeneration*, vol. 22, no. 5, pp. 569–578, Sep. 2014, doi: 10.1111/wrr.12205.

[37] A. C. D. O. Gonzalez, Z. D. A. Andrade, T. F. Costa, and A. R. A. P. Medrado, “Wound healing - A literature review,” *Anais Brasileiros de Dermatologia*, vol. 91, no. 5. Sociedade Brasileira de Dermatologia, pp. 614–620, Sep. 01, 2016. doi: 10.1590/abd1806-4841.20164741.

[38] L. Braiman-Wiksman, I. Solomonik, R. Spira, and T. Tennenbaum, “Novel Insights into Wound Healing Sequence of Events,” *Toxicol Pathol*, vol. 35, no. 6, pp. 767–779, 2007, doi: 10.1080/01926230701584189.

[39] T. Velnar, T. Bailey, and V. Smrkolj, “The wound healing process: An overview of the cellular and molecular mechanisms,” *Journal of International Medical Research*, vol. 37, no. 5. Field House Publishing LLP, pp. 1528–1542, 2009. doi: 10.1177/147323000903700531.

[40] P. Beldon, “Basic science of wound healing,” *Surgery*, vol. 28, no. 9. Elsevier Ltd, pp. 409–412, 2010. doi: 10.1016/j.mpsur.2010.05.007.

[41] B. Gajula, S. Munnamgi, and S. Basu, “How bacterial biofilms affect chronic wound healing: a narrative review,” *International Journal of Surgery: Global Health*, vol. 3, no. 2, pp. e16–e16, Mar. 2020, doi: 10.1097/gh9.0000000000000016.

[42] K. S. Lee, J. J. Wilson, D. P. Rabago, G. S. Baer, J. A. Jacobson, and C. G. Borrero, “Musculoskeletal applications of platelet-rich plasma: Fad or future?,” *American Journal of Roentgenology*, vol. 196, no. 3. pp. 628–636, Mar. 2011. doi: 10.2214/AJR.10.5975.

[43] T. Tolker-Nielsen, “Biofilm Development,” *Microbiol Spectr*, vol. 3, no. 2, Apr. 2015, doi: 10.1128/microbiolspec.mb-0001-2014.

[44] L. K. Vestby, T. Grønseth, R. Simm, and L. L. Nesse, “Bacterial biofilm and its role in the pathogenesis of disease,” *Antibiotics*, vol. 9, no. 2. MDPI AG, Feb. 01, 2020. doi: 10.3390/antibiotics9020059.

[45] H. Katas, M. A. Mohd Akhmar, and S. Suleman Ismail Abdalla, “Biosynthesized silver nanoparticles loaded in gelatine hydrogel for a natural antibacterial and anti-biofilm wound dressing,” *J Bioact Compat Polym*, vol. 36, no. 2, pp. 111–123, Mar. 2021, doi: 10.1177/0883911520988303.

[46] N. Goonoo and A. Bhaw-Luximon, “Nanomaterials combination for wound healing and skin regeneration,” in *Advanced 3D-Printed Systems and Nanosystems for Drug Delivery and Tissue Engineering*, Elsevier, 2020, pp. 159–217. doi: 10.1016/b978-0-12-818471-4.00007-8.

[47] E. A. Kamoun, E. R. S. Kenawy, and X. Chen, “A review on polymeric hydrogel membranes for wound dressing applications: PVA-based hydrogel dressings,” *Journal of Advanced Research*, vol. 8, no. 3. Elsevier B.V., pp. 217–233, May 01, 2017. doi: 10.1016/j.jare.2017.01.005.

[48] E. Rezvani Ghomi, S. Khalili, S. Nouri Khorasani, R. Esmaeely Neisiany, and S. Ramakrishna, “Wound dressings: Current advances and future directions,” *Journal of Applied Polymer Science*, vol. 136, no. 27. John Wiley and Sons Inc., Jul. 15, 2019. doi: 10.1002/app.47738.

[49] G. Dabiri, E. Damstetter, and T. Phillips, “Choosing a Wound Dressing Based on Common Wound Characteristics,” *Advances in Wound Care*, vol.

5, no. 1. Mary Ann Liebert Inc., pp. 32–41, Jan. 01, 2016. doi: 10.1089/wound.2014.0586.

[50] A. E. Stoica, C. Chircov, and A. M. Grumezescu, “Hydrogel dressings for the treatment of burn wounds: An up-to-date overview,” *Materials*, vol. 13, no. 12. MDPI AG, pp. 1–24, Jun. 02, 2020. doi: 10.3390/ma13122853.

[51] J. Zhou *et al.*, “Bacteria-responsive intelligent wound dressing: Simultaneous In situ detection and inhibition of bacterial infection for accelerated wound healing,” *Biomaterials*, vol. 161, pp. 11–23, Apr. 2018, doi: 10.1016/j.biomaterials.2018.01.024.

[52] V. Vivcharenko and A. Przekora, “Modifications of wound dressings with bioactive agents to achieve improved pro-healing properties,” *Applied Sciences (Switzerland)*, vol. 11, no. 9, May 2021, doi: 10.3390/app11094114.

[53] Y. Kong *et al.*, “Degradable tough chitosan dressing for skin wound recovery,” *Nanotechnol Rev*, vol. 9, no. 1, pp. 1576–1585, Jan. 2020, doi: 10.1515/ntrev-2020-0105.

[54] M. Salehi *et al.*, “Naringin-loaded Poly(ε-caprolactone)/Gelatin Electrospun Mat as a Potential Wound Dressing: In vitro and In vivo Evaluation,” *Fibers and Polymers*, vol. 19, no. 1, pp. 125–134, Jan. 2018, doi: 10.1007/s12221-018-7528-6.

[55] K. S. Rho *et al.*, “Electrospinning of collagen nanofibers: Effects on the behavior of normal human keratinocytes and early-stage wound healing,” *Biomaterials*, vol. 27, no. 8, pp. 1452–1461, Mar. 2006, doi: 10.1016/j.biomaterials.2005.08.004.

[56] R. Gobi, P. Ravichandiran, R. S. Babu, and D. J. Yoo, “Biopolymer and synthetic polymer-based nanocomposites in wound dressing applications: A review,” *Polymers*, vol. 13, no. 12. MDPI AG, Jun. 02, 2021. doi: 10.3390/polym13121962.

[57] S. Alven, S. Peter, Z. Mbese, and B. A. Aderibigbe, “Polymer-Based Wound Dressing Materials Loaded with Bioactive Agents: Potential Materials for

the Treatment of Diabetic Wounds," *Polymers*, vol. 14, no. 4. MDPI, Feb. 01, 2022. doi: 10.3390/polym14040724.

[58] M. Maaz Arif *et al.*, "Polymer-based biomaterials for chronic wound management: Promises and challenges," *International Journal of Pharmaceutics*, vol. 598. Elsevier B.V., Apr. 01, 2021. doi: 10.1016/j.ijpharm.2021.120270.

[59] Z. Kalaycıoğlu *et al.*, "Antibacterial nano cerium oxide/chitosan/cellulose acetate composite films as potential wound dressing," *Eur Polym J*, vol. 133, Jun. 2020, doi: 10.1016/j.eurpolymj.2020.109777.

[60] S. A. Shah *et al.*, "Biopolymer-based biomaterials for accelerated diabetic wound healing: A critical review," *International Journal of Biological Macromolecules*, vol. 139. Elsevier B.V., pp. 975–993, Oct. 15, 2019. doi: 10.1016/j.ijbiomac.2019.08.007.

[61] Y. Liu, S. Zhou, Y. Gao, and Y. Zhai, "Electrospun nanofibers as a wound dressing for treating diabetic foot ulcer," *Asian Journal of Pharmaceutical Sciences*, vol. 14, no. 2. Shenyang Pharmaceutical University, pp. 130–143, Mar. 01, 2019. doi: 10.1016/j.ajps.2018.04.004.

[62] G. D. Mogoşanu and A. M. Grumezescu, "Natural and synthetic polymers for wounds and burns dressing," *Int J Pharm*, vol. 463, no. 2, pp. 127–136, Mar. 2014, doi: 10.1016/j.ijpharm.2013.12.015.

[63] N. Sahiner and A. O. Yasar, "The generation of desired functional groups on poly(4-vinyl pyridine) particles by post-modification technique for antimicrobial and environmental applications," *J Colloid Interface Sci*, vol. 402, pp. 327–333, Jul. 2013, doi: 10.1016/j.jcis.2013.03.032.

[64] M. F. Abdullah, T. Nuge, A. Andriyana, B. C. Ang, and F. Muhamad, "Core-Shell fibers: Design, roles, and controllable release strategies in tissue engineering and drug delivery," *Polymers*, vol. 11, no. 12. MDPI AG, Dec. 01, 2019. doi: 10.3390/polym11122008.

[65] Y. Peng *et al.*, "Electrospun PLGA/SF/artemisinin composite nanofibrous membranes for wound dressing," *Int J Biol Macromol*, vol. 183, pp. 68–78, Jul. 2021, doi: 10.1016/j.ijbiomac.2021.04.021.

[66] J. S. Boateng, K. H. Matthews, H. N. E. Stevens, and G. M. Eccleston, "Wound healing dressings and drug delivery systems: A review," *Journal of Pharmaceutical Sciences*, vol. 97, no. 8. John Wiley and Sons Inc., pp. 2892–2923, 2008. doi: 10.1002/jps.21210.

[67] A. M. Croitoru, D. Ficai, A. Ficai, N. Mihailescu, E. Andronescu, and C. F. Turculet, "Nanostructured fibers containing natural or synthetic bioactive compounds in wound dressing applications," *Materials*, vol. 13, no. 10. MDPI AG, May 01, 2020. doi: 10.3390/ma13102407.

[68] J. Artem Ataide, L. Caramori Cefali, F. Machado Croisfelt, A. Arruda Martins Shimojo, L. Oliveira-Nascimento, and P. Gava Mazzola, "Natural actives for wound healing: A review," *Phytotherapy Research*, vol. 32, no. 9. John Wiley and Sons Ltd, pp. 1664–1674, Sep. 01, 2018. doi: 10.1002/ptr.6102.

[69] P. Yudaev, Y. Mezhuev, and E. Chistyakov, "Nanoparticle-Containing Wound Dressing: Antimicrobial and Healing Effects," *Gels*, vol. 8, no. 6. MDPI, Jun. 01, 2022. doi: 10.3390/gels8060329.

[70] M. Rai, A. Yadav, and A. Gade, "Silver nanoparticles as a new generation of antimicrobials," *Biotechnology Advances*, vol. 27, no. 1. pp. 76–83, Jan. 2009. doi: 10.1016/j.biotechadv.2008.09.002.

[71] Z. H. Kareem and A. F. Alkaim, "GREEN SYNTHESIS OF SILVER NANOPARTICLES AND ITS ANTIBACTERIAL ACTIVITY: A REVIEW." [Online]. Available: https://www.researchgate.net/publication/338095757

[72] S. V. Banne, M. S. Patil, R. M. Kulkarni, and S. J. Patil, "Synthesis and Characterization of Silver Nano Particles for EDM Applications," in *Materials Today: Proceedings*, Elsevier Ltd, 2017, pp. 12054–12060. doi: 10.1016/j.matpr.2017.09.130.

[73] M. Georgescu *et al.*, "Natural Compounds for Wound Healing," in *Worldwide Wound Healing - Innovation in Natural and Conventional Methods*, InTech, 2016. doi: 10.5772/65652.

[74] M. Stompor-gorący, A. Bajek-bil, and M. Machaczka, "Chrysin: Perspectives on contemporary status and future possibilities as pro-health agent," *Nutrients*, vol. 13, no. 6. MDPI, Jun. 01, 2021. doi: 10.3390/nu13062038.

[75] S. Naz *et al.*, "Chrysin: Pharmacological and therapeutic properties," *Life Sciences*, vol. 235. Elsevier Inc., Oct. 15, 2019. doi: 10.1016/j.lfs.2019.116797.

[76] A. Luraghi, F. Peri, and L. Moroni, "Electrospinning for drug delivery applications: A review," *Journal of Controlled Release*, vol. 334. Elsevier B.V., pp. 463–484, Jun. 10, 2021. doi: 10.1016/j.jconrel.2021.03.033.

[77] S. P. Miguel *et al.*, "Electrospun polymeric nanofibres as wound dressings: A review," *Colloids and Surfaces B: Biointerfaces*, vol. 169. Elsevier B.V., pp. 60–71, Sep. 01, 2018. doi: 10.1016/j.colsurfb.2018.05.011.

[78] J. Xue, T. Wu, Y. Dai, and Y. Xia, "Electrospinning and electrospun nanofibers: Methods, materials, and applications," *Chemical Reviews*, vol. 119, no. 8. American Chemical Society, pp. 5298–5415, Apr. 24, 2019. doi: 10.1021/acs.chemrev.8b00593.

[79] M. Rahmati *et al.*, "Electrospinning for tissue engineering applications," *Progress in Materials Science*, vol. 117. Elsevier Ltd, Apr. 01, 2021. doi: 10.1016/j.pmatsci.2020.100721.

[80] S. Agarwal, J. H. Wendorff, and A. Greiner, "Use of electrospinning technique for biomedical applications," *Polymer*, vol. 49, no. 26. Elsevier BV, pp. 5603–5621, Dec. 08, 2008. doi: 10.1016/j.polymer.2008.09.014.

[81] M. V. Vellayappan *et al.*, "Electrospinning applications from diagnosis to treatment of diabetes," *RSC Advances*, vol. 6, no. 87. Royal Society of Chemistry, pp. 83638–83655, 2016. doi: 10.1039/c6ra15252j.

[82] A. Haider, S. Haider, and I. K. Kang, "A comprehensive review summarizing the effect of electrospinning parameters and potential applications of nanofibers in biomedical and biotechnology," *Arabian Journal of Chemistry*, vol. 11, no. 8. Elsevier B.V., pp. 1165–1188, Dec. 01, 2018. doi: 10.1016/j.arabjc.2015.11.015.

[83] Z. Li and C. Wang, “Effects of Working Parameters on Electrospinning,” in *SpringerBriefs in Materials*, Springer, 2013, pp. 15–28. doi: 10.1007/978-3-642-36427-3_2.

[84] Y. Qian, X. Zhou, F. Zhang, T. G. H. Diekwisch, X. Luan, and J. Yang, “Triple PLGA/PCL Scaffold Modification including Silver Impregnation, Collagen Coating, and Electrospinning Significantly Improve Biocompatibility, Antimicrobial, and Osteogenic Properties for Orofacial Tissue Regeneration,” *ACS Appl Mater Interfaces*, vol. 11, no. 41, pp. 37381–37396, Oct. 2019, doi: 10.1021/acsami.9b07053.

[85] H. M. Ibrahim, M. M. Reda, and A. Klingner, “Preparation and characterization of green carboxymethylchitosan (CMCS) – Polyvinyl alcohol (PVA) electrospun nanofibers containing gold nanoparticles (AuNPs) and its potential use as biomaterials,” *Int J Biol Macromol*, vol. 151, pp. 821–829, May 2020, doi: 10.1016/j.ijbiomac.2020.02.174.

[86] M. Adeli-Sardou, M. M. Yaghoobi, M. Torkzadeh-Mahani, and M. Dodel, “Controlled release of lawsone from polycaprolactone/gelatin electrospun nano fibers for skin tissue regeneration,” *Int J Biol Macromol*, vol. 124, pp. 478–491, Mar. 2019, doi: 10.1016/j.ijbiomac.2018.11.237.

[87] F. Amini, D. Semnani, S. Karbasi, and S. N. Banitaba, “A novel bilayer drug-loaded wound dressing of PVDF and PHB/Chitosan nanofibers applicable for post-surgical ulcers,” *International Journal of Polymeric Materials and Polymeric Biomaterials*, vol. 68, no. 13, pp. 772–777, Sep. 2019, doi: 10.1080/00914037.2018.1506982.

[88] S. Ahmadian, M. Ghorbani, and F. Mahmoodzadeh, “Silver sulfadiazine-loaded electrospun ethyl cellulose/polylactic acid/collagen nanofibrous mats with antibacterial properties for wound healing,” *Int J Biol Macromol*, vol. 162, pp. 1555–1565, Nov. 2020, doi: 10.1016/j.ijbiomac.2020.08.059.

[89] Z. Hadisi *et al.*, “Hyaluronic Acid (HA)-Based Silk Fibroin/Zinc Oxide Core–Shell Electrospun Dressing for Burn Wound Management,” *Macromol Biosci*, vol. 20, no. 4, Apr. 2020, doi: 10.1002/mabi.201900328.

[90] M. Almukainzi *et al.*, “Co-delivery of gentiopicroside and thymoquinone using electrospun m-PEG/PVP nanofibers: In-vitro and In vivo studies for antibacterial wound dressing in diabetic rats,” *Int J Pharm*, vol. 625, Sep. 2022, doi: 10.1016/j.ijpharm.2022.122106.

[91] D. Gokkaya, M. Topuzogullari, T. Arasoglu, K. Trabzonlu, M. M. Ozmen, and S. Abdurrahmanoğlu, “Antibacterial properties of cationic copolymers as a function of pendant alkyl chain length and degree of quaternization,” *Polym Int*, vol. 70, no. 6, pp. 829–836, Jun. 2021, doi: 10.1002/pi.6170.

[92] T. Hamaki *et al.*, “Isolation of novel bacteria and actinomycetes using soil-extract agar medium,” *J Biosci Bioeng*, vol. 99, no. 5, pp. 485–492, 2005, doi: 10.1263/jbb.99.485.

[93] T. Khampieng, G. E. Wnek, and P. Supaphol, “Electrospun DOXY-h loaded-poly(acrylic acid) nanofiber mats: In vitro drug release and antibacterial properties investigation,” *J Biomater Sci Polym Ed*, vol. 25, no. 12, pp. 1292–1305, Aug. 2014, doi: 10.1080/09205063.2014.929431.

[94] H. Singh *et al.*, “Biomatrix from goat-waste in sponge/gel/powder form for tissue engineering and synergistic effect of nanoceria,” *Biomedical Materials (Bristol)*, vol. 16, no. 2, Mar. 2021, doi: 10.1088/1748-605X/abdb74.

[95] T. Heise, A. Y. Sawyer, T. Hirai, S. Schaible, H. Sy, and S. Wickramasekara, “Report on investigation of ISO 10993–12 extraction conditions,” *Regulatory Toxicology and Pharmacology*, vol. 131, Jun. 2022, doi: 10.1016/j.yrtph.2022.105164.

[96] D. Switha, S. K. Basha, and V. S. Kumari, “In vitro cytocompatibility evaluation of nanostarch reinforced polyaniline-polyvinyl alcohol conductive bionanocomposites for skin tissue engineering application,” *Journal of Umm Al-Qura University for Applied Sciences*, Mar. 2023, doi: 10.1007/s43994-023-00040-x.

[97] S. Qian *et al.*, “Secretory Fluid-Aggregated Janus Electrospun Short Fiber Scaffold for Wound Healing,” *Small*, vol. 18, no. 36, Sep. 2022, doi: 10.1002/smll.202200799.

[98] A. Gõra, M. P. Prabhakaran, G. T. L. Eunice, R. Lakshminarayanan, and S. Ramakrishna, "Silver nanoparticle incorporated poly(l -lactide-co-glycolide) nanofibers: Evaluation of their biocompatibility and antibacterial properties," *J Appl Polym Sci*, vol. 132, no. 42, Nov. 2015, doi: 10.1002/app.42686.

[99] F. Shaikh, Q. K. Panhwar, A. Balouch, S. Ali, W. A. Panhwar, and F. Sheikh, "Synthesis of zinc oxide nanoparticles and their functionalisation with chrysin: exploration of its applications," *Int J Environ Anal Chem*, vol. 102, no. 7, pp. 1662–1671, 2022, doi: 10.1080/03067319.2020.1742889.

[100] C. Liu, Y. Zhu, X. Lun, H. Sheng, and A. Yan, "Effects of wound dressing based on the combination of silver@curcumin nanoparticles and electrospun chitosan nanofibers on wound healing," *Bioengineered*, vol. 13, no. 2, pp. 4328–4339, 2022, doi: 10.1080/21655979.2022.2031415.

[101] C. Liao, Y. Li, and S. C. Tjong, "Antibacterial activities of aliphatic polyester nanocomposites with silver nanoparticles and/or graphene oxide sheets," *Nanomaterials*, vol. 9, no. 8. MDPI AG, Aug. 01, 2019. doi: 10.3390/nano9081102.

[102] F. Rouhollahi, S. A. Hosseini, F. Alihosseini, A. Allafchian, and F. Haghighat, "Investigation on the Biodegradability and Antibacterial Properties of Nanohybrid Suture Based on Silver Incorporated PGA-PLGA Nanofibers," *Fibers and Polymers*, vol. 19, no. 10, pp. 2056–2065, Oct. 2018, doi: 10.1007/s12221-018-8316-7.

[103] S. Samarghandian *et al.*, "Inhibitory and cytotoxic activities of Chrysin on human breast adenocarcinoma cells by induction of apoptosis," *Pharmacogn Mag*, vol. 12, no. 47, pp. S436–S440, 2016, doi: 10.4103/0973-1296.191453.

[104] J. Franková, V. Pivodová, H. Vágnerová, J. Juráňová, and J. Ulrichová, "Effects of silver nanoparticles on primary cell cultures of fibroblasts and keratinocytes in a wound-healing model," *J Appl Biomater Funct Mater*, vol. 14, no. 2, pp. e137–e142, 2016, doi: 10.5301/jabfm.5000268.

PUBLICATIONS FROM THE THESIS

Conference Papers

1. Elif Nur ARSLAN, Serap DERMAN, Murat TOPUZOĞULLARI, "Electrospun Antibacterial Polymer-Metal Composites" 9th Science Days Congress-İstanbul Yeni Yüzyıl University, pp. 76, 2023.